

# Multiple-Source Ellipsoidal Localization Using Acoustic Energy Measurements <sup>★</sup>

Fanqin Meng <sup>a,b</sup>, Xiaojing Shen <sup>c</sup>, Zhiguo Wang <sup>d,e</sup>, Haiqi Liu <sup>c</sup>, Junfeng Wang <sup>a</sup>,  
Yunmin Zhu <sup>c</sup>, Pramod K. Varshney <sup>f</sup>

<sup>a</sup>*School of Aeronautics & Astronautics, Sichuan University, Chengdu, Sichuan 610064, China*

<sup>b</sup>*School of Automation & Information Engineering, Sichuan University of Science & Engineering, Yibin, Sichuan 644000, China*

<sup>c</sup>*School of Mathematics, Sichuan University, Chengdu, Sichuan 610064, China*

<sup>d</sup>*School of Science & Engineering, The Chinese University of Hong Kong, Shenzhen, Guangdong 518172, China*

<sup>e</sup>*Department of Electronic Engineering and Information Science, University of Science and Technology of China, Hefei, Anhui 230026, China.*

<sup>f</sup>*Department of Electrical Engineering & Computer Science, Syracuse University, NY 13244, USA*

---

## Abstract

In this paper, the multiple-source ellipsoidal localization problem based on acoustic energy measurements is investigated via set-membership estimation theory. When the probability density function of measurement noise is unknown-but-bounded, multiple-source localization is a difficult problem since not only the acoustic energy measurements are complicated nonlinear functions of multiple sources, but also the multiple sources bring about a high-dimensional state estimation problem. First, when the energy parameter and the position of the source are bounded in an interval and a ball respectively, the nonlinear remainder bound of the Taylor series expansion is obtained analytically on-line. Next, based on the separability of the nonlinear measurement function, an efficient estimation procedure is developed. It solves the multiple-source localization problem by using an alternating optimization iterative algorithm, in which the remainder bound needs to be known on-line. For this reason, we first derive the remainder bound analytically. When the energy decay factor is unknown but bounded, an efficient estimation procedure is developed based on interval mathematics. Finally, numerical examples demonstrate the effectiveness of the ellipsoidal localization algorithms for multiple-source localization. In particular, our results show that when the noise is non-Gaussian, the set-membership localization algorithm performs better than the EM localization algorithm.

*Key words:* Nonlinear measurements; multiple-source localization; set-membership estimation; acoustic energy measurements.

---

## 1 Introduction

Localization is an important research problem in many systems such as radar, sonar and multimedia systems. Source localization using a network of sensors has far-

reaching applications, e.g., battlefield security, surveillance, environment or health monitoring and disaster relief operations. Many works have investigated the single-source localization problem (see [5], [10], [16], [23], [28]). However, very limited work has been reported on the multiple-source localization problem. In this paper, we focus on the multiple-source localization problem where the aim is to estimate the coordinates of multiple acoustic sources.

The problem of source localization has been addressed by many authors (see papers [5], [10], [16], [23], [28], [29], [30], [33], [38], [39], [41], [44] and books [22], [36], [46]).

---

<sup>★</sup> This work was supported in part by the NSFC No. 61673282, U1836103 and the PCSIRT16R53.

*Email addresses:* mengfanqin2008@163.com (Fanqin Meng), shenxj@scu.edu.cn (Xiaojing Shen), wangzg315@126.com (Zhiguo Wang), haiqiliu0330@163.com (Haiqi Liu), wangjf@scu.edu.cn (Junfeng Wang), ymzhu@scu.edu.cn (Yunmin Zhu), varshney@syr.edu (Pramod K. Varshney).

Most localization methods are based on one of the following three types of physical variables measured by sensor readings for localization: direction of arrival (DOA), time difference of arrival (TDOA) and received sensor signal strength (RSS). DOA can be estimated by exploiting the phase difference measured at receiving sensors (see [43], [47]). TDOA is based upon the difference in arrival times of the emitted signals received at a pair of sensors (see [14], [21], [24]). The source localization estimation task with DOA and TDOA can be performed by solving a nonlinear least squares (NLS) problem. These methods mainly deal with the single target localization problem.

For the multiple-source localization problem, the maximum-likelihood (ML) method is widely used (see [11], [26], [35], [40]). A multiresolution search and the expectation maximization (EM) method [35] were proposed to solve the multiple-source localization problem. An efficient EM algorithm [27] was proposed to improve estimation accuracy. Authors use the model which is called the acoustic energy decay model based on RSS to solve the multiple-source localization problem. The source locations and strengths are estimated using a variant of the EM algorithm in [40] with Helmholtz operator. In this paper, we focus on the acoustic energy decay model mentioned in [11], [26], [35]. The measurement noise is modeled as additive white Gaussian noise in these articles. When the unknown noise is not Gaussian, this approach may lead to poor performance because it is sensitive to the exact probabilistic knowledge of the parameters of noise (see [37]). In practice, the assumed probabilistic model may not be accurate resulting in model mismatch. It then seems more natural to assume that the state perturbations and measurement noise are unknown but bounded (see [31]). Under these assumptions, the articles [7], [15], [17] and [45] discussed the single source localization problem for different applications. However, they do not consider the multiple source localization problem with acoustic energy decay model. These facts motivate us to further research the multiple-source ellipsoidal localization problem under the unknown-but-bounded measurement noise assumption.

When the measurement noise is unknown-but-bounded, set-membership estimation theory may be used to solve the multiple-source localization problem since it does not require a statistical description of the errors. Set-membership estimation was considered first in 1960s (see [4], [32], [42]). The critical step here is the computation of bounding ellipsoids (or boxes, simplexes, parallelepipeds, and polytopes) which are guaranteed to contain the state vector to be estimated given bounds on the perturbations and noises. The problem of bounding ellipsoids has been extensively investigated, for example, see papers [8], [13], [34], the book [18], and references therein. However, the ellipsoidal bounding method has not been investigated for the solution of the multiple-

source localization problem using acoustic energy measurements.

In this paper, we attempt to make progress on the multiple-source localization problem based on acoustic energy measurements in the bounded noise setting by the ellipsoidal bounding estimation method. Multiple-source localization is a difficult problem. There are two main difficulties: the acoustic energy measurements are complicated nonlinear functions of multiple sources and the multiple sources lead to a high-dimensional state estimation problem. The main contributions of this paper are as follows. First, when the parameter is bounded in a convex set, the remainder bound is obtained by taking samples on the boundary of the set. Moreover, when the energy parameter and the position of the source are bounded in an interval and a ball respectively, the remainder bound can be obtained analytically on-line. Next, an efficient procedure is developed to solve the multiple-source localization problem using an alternating optimization iterative algorithm. Furthermore, an efficient estimation procedure is developed based on interval mathematics when the energy decay factor is unknown but bounded. Numerical examples show that when the measurement noise is unknown-but-bounded, the performance of the ellipsoidal localization algorithm is better than that of the EM localization algorithm. Some preliminary results on this problem were presented at a conference [25]. This paper now includes all the mathematical details and proofs.

The rest of this paper is organized as follows. Preliminaries are given in Section 2. In Section 3, the bounding set of the remainder is obtained from the boundary of the state bounding ellipsoid. Moreover, the bounding set is obtained analytically when the energy parameter and the position of the source are bounded in an interval and a ball respectively. In Section 4, the solution to the multiple-source ellipsoidal localization problem is derived by solving an SDP problem based on S-procedure and Schur complement. In Section 5, an interval mathematics estimation method is developed to deal with the multiple-source localization problem when the energy decay factor is unknown but bounded. In Section 6, numerical examples are given and discussed. Finally, Section 7 is devoted to concluding remarks.

## 2 Preliminaries

### 2.1 Acoustic Energy Attenuation Model

The acoustic energy attenuation model is adopted in this paper (see, e.g., [35]). Consider a sensor network composed of  $L$  sensors distributed at known spatial locations, denoted  $r_l$ ,  $l = 1, \dots, L$ , where  $r_l \in \mathbb{R}^d$ ,  $d = 2$  or  $3$ . A fusion center is used to collect the measurement data of the sensors and to run the source localization

algorithm. There are  $N$  acoustic sources whose locations need to be determined. The number of sources  $N$  is known. The sources are static and the locations of the sources are denoted by  $\rho_n \in \mathbb{R}^d$ ,  $n = 1, \dots, N$ , which are unknown. Each sensor considers only a single RSS measurement and it is expressed as

$$y_l = g_l \sum_{n=1}^N \frac{s_n}{\|\rho_n - r_l\|^\alpha} + \varepsilon_l, \quad l = 1, \dots, L, \quad (1)$$

where  $s_n$  is a scalar denoting the energy emitted by the  $n$ -th source,  $\|\rho_n - r_l\| \neq 0$  is the distance between the  $n$ -th source and the  $l$ -th sensor,  $g_l$  is the gain factor of the  $l$ -th acoustic sensor,  $\alpha$  is a known energy decay factor with a typical value lies between 2 to 4 (see [27]), and the additive measurement noises  $\varepsilon_l$ ,  $l = 1, \dots, L$ , are independent and unknown-but-bounded, i.e.,  $\varepsilon = [\varepsilon_1, \varepsilon_2, \dots, \varepsilon_L]^T$  is confined to a specified box

$$\mathcal{B}^\varepsilon = \{\varepsilon \in \mathbb{R}^L : \mathbf{D}_l^\varepsilon \leq \varepsilon_l \leq \mathbf{U}_l^\varepsilon, l = 1, \dots, L\}, \quad (2)$$

where  $\mathbf{D}_l^\varepsilon$  is the  $l$ -th component of the lower bound  $\mathbf{D}^\varepsilon$  of the box  $\mathcal{B}^\varepsilon$ , i.e.,  $\mathbf{D}^\varepsilon = [\mathbf{D}_1^\varepsilon, \dots, \mathbf{D}_L^\varepsilon]^T$ ,  $\mathbf{U}_l^\varepsilon$  is the  $l$ -th component of the upper bound  $\mathbf{U}^\varepsilon$  of the box  $\mathcal{B}^\varepsilon$ , i.e.,  $\mathbf{U}^\varepsilon = [\mathbf{U}_1^\varepsilon, \dots, \mathbf{U}_L^\varepsilon]^T$ , and  $[\cdot]^T$  denotes the transpose of  $[\cdot]$ .

Moreover, the scalar  $s_n$  is independent of the position  $\rho_n$  of the  $n$ -th source and the unknown parameters of the different sources are independent. The unknown parameters of the  $n$ -th source are  $s_n$  and  $\rho_n$ , which are denoted as  $\mathbf{x}_n$ , i.e.,  $\mathbf{x}_n = [s_n, \rho_n^T]^T$ ,  $n = 1, \dots, N$ . All the unknown parameters of the  $N$  sources are concatenated and denoted as  $\mathbf{x} = [\mathbf{x}_1^T, \mathbf{x}_2^T, \dots, \mathbf{x}_N^T]^T$ . All the measurements of the  $L$  sensors are denoted as  $\mathbf{y} = [y_1, y_2, \dots, y_L]^T$ . We define the following notation:

$$f(\mathbf{x}) = \left[ \sum_{n=1}^N f_{n,1}(\mathbf{x}_n), \dots, \sum_{n=1}^N f_{n,L}(\mathbf{x}_n) \right]^T, \quad (3)$$

where  $f_{n,l}(\mathbf{x}_n) = g_l \frac{s_n}{\|\rho_n - r_l\|^\alpha}$ . The acoustic energy measurement functions (1) used for multi-source localization are written in a simpler notation as

$$\mathbf{y} = f(\mathbf{x}) + \varepsilon, \quad (4)$$

where  $\varepsilon = [\varepsilon_1, \varepsilon_2, \dots, \varepsilon_L]^T$  is the additive measurement noise.

## 2.2 Multiple-source Ellipsoidal Localization Problem

The bounding set  $\mathcal{E}$  of the state  $\mathbf{x}$  of the  $N$  sources is considered as the Cartesian product of  $\mathcal{E}_n$ , i.e.,

$$\mathcal{E} = \prod_{n=1}^N \mathcal{E}_n, \quad (5)$$

where  $\mathcal{E}_n$  is the bounding set of the state  $\mathbf{x}_n$ . Since the scalar  $s_n$  is independent of the position  $\rho_n$  of the  $n$ -th source,  $s_n$  is contained in an interval  $\mathcal{E}_n^s = \{s \in \mathbb{R}^1 : |s - \hat{s}_n| \leq S_n\}$  and  $\rho_n$  is contained in an ellipsoid

$$\mathcal{E}_n^\rho = \{\rho \in \mathbb{R}^d : (\rho - \hat{\rho}_n)^T \mathbf{P}_n^{-1} (\rho - \hat{\rho}_n) \leq 1\},$$

where  $\hat{\rho}_n$  is the center of the ellipsoid  $\mathcal{E}_n^\rho$ , and  $\mathbf{P}_n$  is the *shape matrix* of the ellipsoid  $\mathcal{E}_n^\rho$ . Then the bounding set  $\mathcal{E}_n$  is

$$\mathcal{E}_n = \mathcal{E}_n^s \times \mathcal{E}_n^\rho. \quad (6)$$

When the nonlinear measurement function  $f$  is linearized, the remainder term is bounded by a box. Specifically, by Taylor's Theorem,  $f$  is linearized to

$$f(\mathbf{x}) = f(\hat{\mathbf{x}}) + \mathbf{J}(\hat{\mathbf{x}})(\mathbf{x} - \hat{\mathbf{x}}) + \Delta f(\mathbf{x}, \hat{\mathbf{x}}), \quad (7)$$

where  $\hat{\mathbf{x}} = [\hat{\mathbf{x}}_1^T, \dots, \hat{\mathbf{x}}_N^T]^T$ ,  $\hat{\mathbf{x}}_n = [\hat{s}_n, \hat{\rho}_n^T]^T$ ,  $n = 1, \dots, N$ ,  $\mathbf{J}(\hat{\mathbf{x}}) = \frac{\partial f(\mathbf{x})}{\partial \mathbf{x}}|_{\hat{\mathbf{x}}}$  is the Jacobian matrix, and  $\Delta f(\mathbf{x}, \hat{\mathbf{x}})$  is the higher-order remainder which is bounded in a box  $\mathcal{B}$  for all  $\mathbf{x} \in \mathcal{E}$ , i.e.,

$$\Delta f(\mathbf{x}, \hat{\mathbf{x}}) \in \mathcal{B} = \{\mathbf{z} \in \mathbb{R}^L : \mathbf{D}_l^f \leq \mathbf{z}_l \leq \mathbf{U}_l^f, l = 1, \dots, L\}, \quad (8)$$

where  $\mathbf{D}_l^f$  is the  $l$ -th component of the lower bound  $\mathbf{D}^f$  of the box  $\mathcal{B}$ , i.e.,  $\mathbf{D}^f = [\mathbf{D}_1^f, \dots, \mathbf{D}_L^f]^T$ ,  $\mathbf{U}_l^f$  is the  $l$ -th component of the upper bound  $\mathbf{U}^f$  of the box  $\mathcal{B}$ , i.e.,  $\mathbf{U}^f = [\mathbf{U}_1^f, \dots, \mathbf{U}_L^f]^T$ . Note that we do not assume that the box  $\mathcal{B}$  is given before the algorithm. It is determined on-line.

We consider an efficient estimation procedure to solve the multiple-source localization problem by using an alternating optimization iterative approach. It is formulated as follows. Assume that the state  $\mathbf{x}$  belongs to a given initial bounding set  $\mathcal{E}^0$ , which is the Cartesian product of ellipsoids  $\mathcal{E}_n^0$ ,  $n = 1, \dots, N$ , i.e.,

$$\mathcal{E}^0 = \prod_{n=1}^N \mathcal{E}_n^0 = \prod_{n=1}^N \mathcal{E}_n^{s,0} \times \mathcal{E}_n^{\rho,0}, \quad (9)$$

where  $\mathcal{E}_n^{s,0} = \{s \in \mathbb{R}^1 : |s - \hat{s}_n^0| \leq S_n^0\}$ , and  $\mathcal{E}_n^{\rho,0} = \{\rho \in \mathbb{R}^d : (\rho - \hat{\rho}_n^0)^T (\mathbf{P}_n^0)^{-1} (\rho - \hat{\rho}_n^0) \leq 1\}$ .

At the  $i$ -th iteration, given that  $\mathbf{x}$  belongs to the current bounding set  $\mathcal{E}^i$ ,

$$\mathcal{E}^i = \prod_{n=1}^N \mathcal{E}_n^i = \prod_{n=1}^N \mathcal{E}_n^{s,i} \times \mathcal{E}_n^{\rho,i}, \quad (10)$$

where  $\mathcal{E}_n^{s,i} = \{s \in \mathbb{R}^1 : |s - \hat{s}_n^i| \leq S_n^i\}$ , and  $\mathcal{E}_n^{\rho,i} = \{\rho \in \mathbb{R}^d : (\rho - \hat{\rho}_n^i)^T (\mathbf{P}_n^i)^{-1} (\rho - \hat{\rho}_n^i) \leq 1\}$ .

At the  $(i+1)$ -th iteration, based on the measurement  $\mathbf{y}$ , the goal of the ellipsoidal localization estimation algorithm is to determine a bounding set  $\mathcal{E}^{i+1} = \prod_{n=1}^N \mathcal{E}_n^{i+1}$ , whenever I)  $\mathbf{x}$  is in  $\mathcal{E}^i$ , II) the measurement noise  $\boldsymbol{\varepsilon} \in \mathcal{B}^\varepsilon$  and the remainder  $\Delta f(\mathbf{x}, \hat{\mathbf{x}}^i) \in \mathcal{B}^i$ .

Moreover, the shape matrix of the state bounding set  $\mathcal{E}^i$  is denoted as  $\mathbf{P}^i$  and

$$\mathbf{P}^i = \begin{bmatrix} \mathbf{P}_1^i & 0 & 0 & 0 & \cdots & 0 & 0 \\ 0 & s_1^i & 0 & 0 & \cdots & 0 & 0 \\ 0 & 0 & \mathbf{P}_2^i & 0 & \cdots & 0 & 0 \\ 0 & 0 & 0 & s_2^i & \cdots & 0 & 0 \\ \vdots & \vdots & \vdots & \vdots & \vdots & \vdots & \vdots \\ 0 & 0 & 0 & 0 & \cdots & \mathbf{P}_N^i & 0 \\ 0 & 0 & 0 & 0 & \cdots & 0 & s_N^i \end{bmatrix}.$$

We provide a state bounding set  $\mathcal{E}^i$  by minimizing its “size” at  $i$ -th iteration which is a function of the shape matrix  $\mathbf{P}^i$  denoted by  $g(\mathbf{P}^i)$ . Throughout this paper,  $g(\mathbf{P}^i)$  is the trace function, i.e.,  $g(\mathbf{P}^i) = \text{trace}(\mathbf{P}^i)$ . The algorithm terminates when the decrease of  $g(\mathbf{P}^{i+1})$  is sufficiently small, i.e.,  $g(\mathbf{P}^i) - g(\mathbf{P}^{i+1}) \leq \delta$ , where  $\delta$  is a small positive scalar. In general, the value of  $\delta$  should be chosen on a case-by-case basis based on prior information or numerical simulations.

**Remark 1** *Since the sources are static, the proposed method can be extended to multiple measurements in a straightforward manner using a recursive approach. That is, based on the past measurements, we can derive a bounding set of the state which may be used as the initial value of the algorithm. Moreover, the state bounding set is updated based on the initial state bounding set and the new measurement.*

**Remark 2** *The number of sources has to be known in advance in this paper. In most studies of the multiple-source localization problem, the number of sources is assumed known ([12], [35], [40]). When the number of sources is unknown, the basic idea is to select an optimization criterion to determine the number of sources.*

### 3 Bounding the Remainder

In this section, we consider the problem of determining a bounding box to cover the higher-order remainder. The bounding box of the remainder is derived at each iteration based on the boundary of the convex bounding set of the state. In particular, when the energy parameter and the position of each source are bounded in an interval

and a ball respectively, the remainder bound is obtained analytically.

As shown in Equation (3), the measurement function  $f$  is rewritten as a state separable equation:

$$f = \sum_{n=1}^N f_n(\mathbf{x}_n), \quad (11)$$

where  $f_n(\mathbf{x}_n) = [f_{n,1}(\mathbf{x}_n), \dots, f_{n,L}(\mathbf{x}_n)]^T$ ,  $\mathbf{x}_n \in \mathbb{R}^{d+1}$  is the state parameter of the  $n$ -th source. The derivative function of  $f$  satisfies  $\frac{\partial f(\mathbf{x})}{\partial \mathbf{x}_n} = \frac{\partial f_n(\mathbf{x}_n)}{\partial \mathbf{x}_n}$ . Thus, we have

$$\begin{aligned} \mathbf{J}(\hat{\mathbf{x}}^i) &= \left[ \frac{\partial f(\mathbf{x})}{\partial \mathbf{x}_1}, \dots, \frac{\partial f(\mathbf{x})}{\partial \mathbf{x}_N} \right]_{\hat{\mathbf{x}}^i} \\ &= \left[ \frac{\partial f_1(\mathbf{x}_1)}{\partial \mathbf{x}_1} \Big|_{\hat{\mathbf{x}}_1^i}, \dots, \frac{\partial f_N(\mathbf{x}_N)}{\partial \mathbf{x}_N} \Big|_{\hat{\mathbf{x}}_N^i} \right]. \end{aligned} \quad (12)$$

The remainder in (7) is rewritten as

$$\Delta f(\mathbf{x}, \hat{\mathbf{x}}^i) = f(\mathbf{x}) - f(\hat{\mathbf{x}}) - \mathbf{J}(\hat{\mathbf{x}}^i)(\mathbf{x} - \hat{\mathbf{x}}^i). \quad (13)$$

Substituting (11) and (12) into (13), the remainder is

$$\Delta f(\mathbf{x}, \hat{\mathbf{x}}^i) = \sum_{n=1}^N (f_n(\mathbf{x}_n) - f_n(\hat{\mathbf{x}}_n^i) - \mathbf{J}_n(\hat{\mathbf{x}}_n^i)(\mathbf{x}_n - \hat{\mathbf{x}}_n^i)). \quad (14)$$

where  $\mathbf{J}_n(\hat{\mathbf{x}}_n^i) = \frac{\partial f_n(\mathbf{x}_n)}{\partial \mathbf{x}_n} \Big|_{\hat{\mathbf{x}}_n^i}$  and  $\mathbf{x}_n \in \mathcal{E}_n^i$ ,  $n = 1, \dots, N$ . Denote

$$\begin{aligned} \Delta f_n(\mathbf{x}_n, \hat{\mathbf{x}}_n^i) &= f_n(\mathbf{x}_n) - \mathbf{J}_n(\hat{\mathbf{x}}_n^i)(\mathbf{x}_n - \hat{\mathbf{x}}_n^i) \\ &\quad - f_n(\hat{\mathbf{x}}_n^i), n = 1, \dots, N, \end{aligned} \quad (15)$$

where

$$\Delta f_n(\mathbf{x}_n, \hat{\mathbf{x}}_n^i) = [\Delta f_{n,1}(\mathbf{x}_n, \hat{\mathbf{x}}_n^i), \dots, \Delta f_{n,L}(\mathbf{x}_n, \hat{\mathbf{x}}_n^i)]^T.$$

If there is a box  $\mathcal{B}_n^i$  which contains  $\Delta f_n(\mathbf{x}_n, \hat{\mathbf{x}}_n^i)$  for all  $\mathbf{x}_n \in \mathcal{E}_n^i$ , i.e.,

$$\begin{aligned} \Delta f_n(\mathbf{x}_n, \hat{\mathbf{x}}_n^i) \in \mathcal{B}_n^i &= \{z \in \mathbb{R}^L : \mathbf{D}_{n,l}^i \leq z_l \\ &\leq \mathbf{U}_{n,l}^i, l = 1, 2, \dots, L\}, \end{aligned} \quad (16)$$

where  $\mathbf{D}_{n,l}^i$  is the  $l$ -th component of the lower bound  $\mathbf{D}_n^i$  of the box  $\mathcal{B}_n^i$ , i.e.,  $\mathbf{D}_n^i = [\mathbf{D}_{n,1}^i, \dots, \mathbf{D}_{n,L}^i]^T$ ,  $\mathbf{U}_{n,l}^i$  is the  $l$ -th component of the upper bound  $\mathbf{U}_n^i$  of the box  $\mathcal{B}_n^i$ , i.e.,  $\mathbf{U}_n^i = [\mathbf{U}_{n,1}^i, \dots, \mathbf{U}_{n,L}^i]^T$ , then the bounding box  $\mathcal{B}^i$  (see (8)) of the remainder  $\Delta f(\mathbf{x}, \hat{\mathbf{x}}^i)$  is derived with the

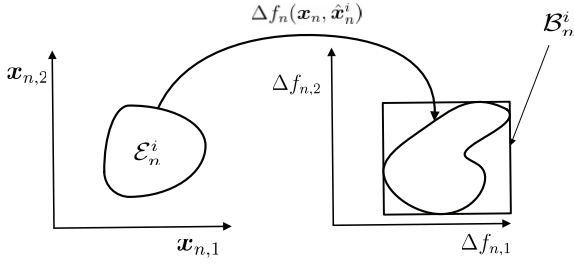


Fig. 1. The bounding box  $\mathcal{B}_n^i$  of  $\Delta f(\mathbf{x}, \hat{\mathbf{x}}^i)$ .

lower bound and upper bound as follows:

$$\mathbf{D}^{f,i} = \sum_{n=1}^N \mathbf{D}_n^i, \quad \mathbf{U}^{f,i} = \sum_{n=1}^N \mathbf{U}_n^i. \quad (17)$$

The compact bounding box  $\mathcal{B}_n^i$  of the remainder set  $\{\Delta f_n(\mathbf{x}_n, \hat{\mathbf{x}}_n^i), \mathbf{x}_n \in \mathcal{E}_n^i\}$ , as shown in Fig. 1 ( $L = 2$ ), can be equivalently used the following optimization problems, for  $l = 1, \dots, L$ ,

$$\begin{aligned} & \max t \\ & \text{subject to } t \leq \Delta f_{n,l}(\mathbf{x}_n, \hat{\mathbf{x}}_n^i), \quad \mathbf{x}_n \in \mathcal{E}_n^i, \end{aligned} \quad (18)$$

and

$$\begin{aligned} & \min t \\ & \text{subject to } t \geq \Delta f_{n,l}(\mathbf{x}_n, \hat{\mathbf{x}}_n^i), \quad \mathbf{x}_n \in \mathcal{E}_n^i. \end{aligned} \quad (19)$$

Since there are infinite number of constraints, the problem (18)-(19) is a semi-infinite optimization problem [6]. In general, it is an NP-hard problem. In order to reduce the computational complexity, we have the following result on finding the bounds of the remainder.

**Proposition 1** *At  $i$ -th iteration, the parameter of the  $n$ -th source is contained in a closed convex set  $\mathcal{E}_n^i$ , i.e.,  $[s_n, \rho_n^T]^T \in \mathcal{E}_n^i$  defined in (6), the bounds of the remainder  $\Delta f_{n,l}(\mathbf{x}_n, \hat{\mathbf{x}}_n^i)$  are obtained as follows:*

(a) *If the  $l$ -th sensor is not contained in the set  $\mathcal{E}_n^{\rho,i}$ , then the minimum and maximum of  $\Delta f_{n,l}(\mathbf{x}_n, \hat{\mathbf{x}}_n^i)$  are obtained at the stationary point  $\hat{\mathbf{x}}_n^i$  or on the boundary of  $\mathcal{E}_n^i$ .*

(b) *If the  $l$ -th sensor is contained in the set  $\mathcal{E}_n^{\rho,i}$ , then the maximum of  $\Delta f_{n,l}(\mathbf{x}_n, \hat{\mathbf{x}}_n^i)$  is  $+\infty$  and the minimum  $\Delta f_{n,l}(\mathbf{x}_n, \hat{\mathbf{x}}_n^i)$  is obtained at the stationary point  $\hat{\mathbf{x}}_n^i$  or on the boundary of  $\mathcal{E}_n^i$ .*

**PROOF.** See the Appendix.

**Remark 3** *Proposition 1 means that when we determine the remainder bound, only the boundary of the set  $\mathcal{E}_n^i$  and the stationary point  $\hat{\mathbf{x}}_n^i$  are useful. It is not necessary to consider the other interior points of the set  $\mathcal{E}_n^i$  except the stationary point  $\hat{\mathbf{x}}_n^i$ . Thus, the computational complexity is reduced quite significantly. When we take samples from the boundary of the set  $\mathcal{E}_n^i$ , they are sufficient to derive the outer bounding box of the remainder set.*

**Remark 4** *To guarantee that the resulting box actually contains the true remainder set, we can heuristically enlarge the sampling area, such as taking samples from the boundary of the larger set  $1.1 \cdot \mathcal{E}_n^i = 1.1 \cdot \mathcal{E}_n^{s,i} \times 1.1 \cdot \mathcal{E}_n^{\rho,i}$ , where  $1.1 \cdot \mathcal{E}_n^{s,i} = \{s_n \in \mathbb{R}^1 : |s_n - \hat{s}_n^i| \leq 1.1 \cdot S_n^i\}$ ,  $1.1 \cdot \mathcal{E}_n^{\rho,i} = \{\rho \in \mathbb{R}^d : (\rho - \hat{\rho}_n^i)^T (\mathbf{P}_n^i)^{-1} (\rho - \hat{\rho}_n^i) \leq (1.1)^2\}$ , then the remainder set becomes a little larger than that based on  $\mathbf{x}_n \in \mathcal{E}_n^i$ . If we derive a box to cover the little larger remainder, then this box can cover the original remainder set  $\{\Delta f_n(\mathbf{x}_n, \hat{\mathbf{x}}_n^i), \mathbf{x}_n \in \mathcal{E}_n^i\}$ .*

Furthermore, if  $s_n$  is contained in the interval  $\mathcal{E}_n^{s,i} = \{s_n \in \mathbb{R}^1 : |s_n - \hat{s}_n^i| \leq S_n^i\}$  and  $\rho_n$  is contained in the ball  $\mathcal{E}_n^{\rho,i} = \{\rho_n \in \mathbb{R}^d : \|\rho_n - \hat{\rho}_n^i\| \leq R_n^i\}$  as defined in (6), then the remainder bound is obtained analytically as stated in the following propositions.

**Proposition 2** *If the energy parameter and the position of the source are bounded in an interval and a ball respectively, i.e.,  $\mathbf{x}_n \in \mathcal{E}_n^i = \mathcal{E}_n^{s,i} \times \mathcal{E}_n^{\rho,i}$ ,  $\mathcal{E}_n^{s,i} = \{s_n \in \mathbb{R}^1 : |s_n - \hat{s}_n^i| \leq S_n^i\}$  and  $\mathcal{E}_n^{\rho,i} = \{\rho_n \in \mathbb{R}^d : \|\rho_n - \hat{\rho}_n^i\| \leq R_n^i\}$ , and the sensors are not contained in the state bounding set, i.e.,  $R_n^i < \min\{\tau_l = \|\hat{\rho}_n^i - r_l\| : l = 1, \dots, L\}$ , where  $r_l$ ,  $\hat{\rho}_n^i$  and  $\alpha > 0$  are defined in (1), then the bounding box  $\mathcal{B}_n^i$  of the remainder  $\Delta f_n(\mathbf{x}_n, \hat{\mathbf{x}}_n^i)$ , is obtained analytically, i.e., the maximum and minimum of function  $\Delta f_{n,l}(\mathbf{x}_n, \hat{\mathbf{x}}_n^i)$ , for  $l = 1, \dots, L$ , are*

$$\begin{aligned} \max_{\mathbf{x}_n \in \mathcal{E}_n^i} f_{n,l}(\mathbf{x}_n, \hat{\mathbf{x}}_n^i) &= \max \left\{ \Delta \tilde{f}_{n,l}(1, -S_n^i, R_n^i), \right. \\ & \left. \Delta \tilde{f}_{n,l}(-1, S_n^i, R_n^i), \Delta \tilde{f}_{n,l}(-1, -S_n^i, R_n^i), 0 \right\}, \end{aligned} \quad (20)$$

$$\begin{aligned} \min_{\mathbf{x}_n \in \mathcal{E}_n^i} \Delta f_{n,l}(\mathbf{x}_n, \hat{\mathbf{x}}_n^i) &= \min \left\{ \Delta \tilde{f}_{n,l}(-1, -S_n^i, t_1), \right. \\ & \Delta \tilde{f}_{n,l}(1, S_n^i, t_2), \Delta \tilde{f}_{n,l}(\max\{-1, \hat{k}_1\}, -S_n^i, R_n^i), \\ & \left. \Delta \tilde{f}_{n,l}(\max\{-1, \min\{\hat{k}_2, 1\}\}, S_n^i, R_n^i), 0 \right\}, \end{aligned} \quad (21)$$

where

$$\begin{aligned} \Delta \tilde{f}_{n,l}(k, \Delta s_n, t) &= g_l \left( \frac{\hat{s}_n^i + \Delta s_n}{(t^2 + \tau_l^2 + 2t\tau_l k)^{\alpha/2}} + \frac{\alpha \hat{s}_n^i t k}{\tau_l^{\alpha+1}} \right. \\ & \left. - \frac{\hat{s}_n^i + \Delta s_n}{\tau_l^\alpha} \right), \end{aligned}$$

is a function of variables  $k, \Delta s$  and  $t$ .

$$t_1 = \min\left\{\tau_l \left(1 - \left(1 - \frac{S_n^i}{\hat{s}_n^i}\right)^{1/(\alpha+1)}\right), R_n^i\right\}, \quad (22)$$

$$t_2 = \min\left\{\tau_l \left(1 + \frac{S_n^i}{\hat{s}_n^i}\right)^{1/(\alpha+1)} - 1, R_n^i\right\}, \quad (23)$$

$$\hat{k}_1 = \frac{\left(1 - \frac{S_n^i}{\hat{s}_n^i}\right)^{1/(\alpha/2+1)} - 1}{2R_n^i \tau_l} \tau_l^2 - (R_n^i)^2, \quad (24)$$

$$\hat{k}_2 = \frac{\left(1 + \frac{S_n^i}{\hat{s}_n^i}\right)^{1/(\alpha/2+1)} - 1}{2R_n^i \tau_l} \tau_l^2 - (R_n^i)^2. \quad (25)$$

**PROOF.** See the Appendix.

**Remark 5** Proposition 2 means that when the energy parameter and the position of the source are bounded in an interval and a ball respectively, the bounding box of the remainder is obtained analytically. The upper and lower bounds of the bounding box  $\mathcal{B}_n^i$ , for  $l = 1, \dots, L$ , are

$$\begin{aligned} D_{n,l}^i &= \min_{\mathbf{x}_n \in \mathcal{E}_n} \Delta f_{n,l}(\mathbf{x}_n, \hat{\mathbf{x}}_n^i), \\ U_{n,l}^i &= \max_{\mathbf{x}_n \in \mathcal{E}_n} \Delta f_{n,l}(\mathbf{x}_n, \hat{\mathbf{x}}_n^i). \end{aligned}$$

Obviously, the computational complexity of finding the remainder bound is significantly reduced due to the availability of the analytical solution.

In Proposition 2, we have assumed that the set  $\mathcal{E}_n^{\rho,i}$  does not contain any sensor. If this assumption is not satisfied, we have the following result.

**Proposition 3** If the energy parameter and the position of the source are bounded in an interval and a ball respectively, as shown in Proposition 2, and the  $l$ -th sensor is contained in the state bounding set, i.e.,  $R_n > \tau_l = \|\hat{\rho}_n^i - r_l\|$ , where  $r_l, \hat{\rho}_n^i$  and  $\alpha > 0$  are defined in (1), the minimum of the remainder  $\Delta f_{n,l}(\mathbf{x}_n, \hat{\mathbf{x}}_n^i)$  is

$$\begin{aligned} \min_{\mathbf{x}_n \in \mathcal{E}_n^i} \Delta f_{n,l}(\mathbf{x}_n, \hat{\mathbf{x}}_n^i) &= g_l \min \left\{ \Delta \tilde{f}_{n,l}(-1, -S_n^i, t_1^-), \right. \\ &\quad \Delta \tilde{f}_{n,l}(1, S_n^i, t_2^-), \Delta \tilde{f}_{n,l}(\hat{k}_1, -S_n^i, R_n^i), \\ &\quad \left. \Delta \tilde{f}_{n,l}(\hat{k}_2, S_n^i, R_n^i), 0 \right\}, \end{aligned} \quad (26)$$

where  $\Delta \tilde{f}_{n,l}(k, \Delta s, t)$ ,  $\hat{k}_1$  and  $\hat{k}_2$  are same as that in

Proposition 2, and

$$t_1^- = \tau_l \left(1 - \left(1 - \frac{S_n^i}{\hat{s}_n^i}\right)^{1/(\alpha+1)}\right),$$

$$t_2^- = \tau_l \left(1 + \frac{S_n^i}{\hat{s}_n^i}\right)^{1/(\alpha+1)} - 1.$$

**PROOF.** See the Appendix.

**Remark 6** It is easy to find that when  $R_n > \tau_l$ ,  $\max_{\mathbf{x}_n \in \mathcal{E}_n^i} \Delta f_{n,l}(\mathbf{x}_n, \hat{\mathbf{x}}_n^i) = +\infty$ . It means that the remainder cannot be covered by a bounded box. In this case, the remainder is constrained by a hyperplane.

## 4 Multiple-source Ellipsoidal Localization Algorithm

In this section, we derive the multiple-source ellipsoidal localization method. The main idea is that based on the separability of the nonlinear measurement function, an S-procedure estimation method is developed to deal with the multiple-source localization problem by using an alternating optimization iterative algorithm.

For multiple-source localization, the bounding box  $\mathcal{B}_n^i$  (see (16)) of the remainder  $\Delta f_n$ , for  $n = 1, \dots, N$ , is derived based on the current bounding set of the  $n$ -th source state by Proposition 1 or Propositions 2-3, at the  $i$ -th iteration. The bounding box  $\mathcal{B}^i$  of the remainder  $\Delta f$  is derived based on the bounding boxes  $\mathcal{B}_n^i$ ,  $n = 1, \dots, N$ , as shown in (17). The set  $\{1, \dots, L\}$  is divided into two disjoint subsets  $\mathcal{L}^{+,i}$  and  $\mathcal{L}^{-,i}$ ,

$$\mathcal{L}^{+,i} = \{l : U_l^{f,i} < +\infty, l = 1, \dots, L\}, \quad (27)$$

$$\mathcal{L}^{-,i} = \{l : U_l^{f,i} = +\infty, l = 1, \dots, L\}. \quad (28)$$

Moreover, we use the current state bound  $\mathcal{E}_1^i \times \dots \times \mathcal{E}_N^i$  and the remainder bound  $\mathcal{B}_1^i \times \dots \times \mathcal{B}_N^i$  to determine the bounding set of the state at  $(i+1)$ -th iteration, i.e., look for  $\hat{\rho}_n^{i+1}, \hat{s}_n^{i+1}, S_n^{i+1}$  and  $\mathbf{P}_n^{i+1}$  of  $\mathcal{E}_n^{i+1}$  such that the state  $\mathbf{x}_n$  of the  $n$ -th source belongs to  $\mathcal{E}_n^{i+1}$ ,  $n = 1, \dots, N$ . It is obtained by the following proposition.

**Proposition 4** At  $(i+1)$ -th iteration, based on measurement  $\mathbf{y}$ , the current state bound  $\mathcal{E}_1^i \times \dots \times \mathcal{E}_N^i$ , the current remainder bound  $\mathcal{B}_1^i \times \dots \times \mathcal{B}_N^i$ , and the noise bounding box  $\mathcal{B}^e$ , for the  $n$ -th source state  $\mathbf{x}_n$ ,  $n = 1, \dots, N$ , we have:

(a) The state bounding set  $\mathcal{E}_n^{s,(i+1)}$ , as shown in (10), is obtained by solving the optimization problem in the variables  $(S_n^{i+1})^2, \hat{s}_n^{i+1}$ , nonnegative scalars  $\tau_j^1 \geq 0, \tau_j^2 \geq$

$0, j = 1, \dots, N, \tau_l^+ \geq 0, l \in \mathcal{L}^{+,i}, \tau_l^- \geq 0, l \in \mathcal{L}^{-,i},$

$$\min (S_n^{i+1})^2 \quad (29)$$

subject to

$$\begin{aligned} -\tau_j^1 &\leq 0, -\tau_j^2 \leq 0, j = 1, \dots, N, \\ -\tau_l^+ &\leq 0, l \in \mathcal{L}^{+,i}, -\tau_l^- \leq 0, l \in \mathcal{L}^{-,i}, \end{aligned} \quad (30)$$

$$\begin{bmatrix} -(S_n^{i+1})^2 \\ (\Phi_n^{s,(i+1)}(\Psi^{+, (i+1)})_{\perp})^T \\ \Phi_n^{s,(i+1)}(\Psi^{+, (i+1)})_{\perp} \\ -(\Psi^{+, (i+1)})_{\perp}^T \Xi_n(\Psi^{+, (i+1)})_{\perp} \end{bmatrix} \preceq 0, \quad (31)$$

where

$$\Phi_n^{s,(i+1)} = [\hat{s}_n^i - \hat{s}_n^{i+1}, \mathbf{I}_n^T \hat{\mathbf{E}}^i, 0, 0], \quad (32)$$

$$\begin{aligned} \Psi^{+, (i+1)} &= [f^+(\hat{\mathbf{x}}^i) + \hat{\mathbf{e}}^+, \mathbf{e}^{\varepsilon,+} - \mathbf{y}^+, \mathbf{J}^{+,i} \hat{\mathbf{E}}^i, \\ &\quad \text{diag}(\frac{\hat{\mathbf{b}}^{+,i} + \mathbf{b}^{\varepsilon,+}}{2})], \end{aligned} \quad (33)$$

$$\Psi_l^{-, (i+1)} = \begin{bmatrix} H_l & \frac{1}{2} \mathbf{J}_l^i \hat{\mathbf{E}}^i & \mathbf{0} \\ \frac{1}{2} (\mathbf{J}_l^i \hat{\mathbf{E}}^i)^T & \mathbf{0} & \mathbf{0} \\ \mathbf{0} & \mathbf{0} & \mathbf{0} \end{bmatrix}, \quad (34)$$

$$H_l = f_l(\hat{\mathbf{x}}^i) + \mathbf{e}_l^{\varepsilon} - \frac{b_l^{\varepsilon}}{2} + D_l^{f,i} - \mathbf{y}_l, \quad l \in \mathcal{L}^{-,i}, \quad (35)$$

the  $n$ -th entry is  $\mathbf{I}_1$

$\mathbf{I}_n^1 = [0, \dots, \mathbf{I}_1, \dots, 0]$ ,  $\mathbf{I}_1 = [1 \ \mathbf{0}]$ ,  $\mathbf{0} \in \mathbb{R}^{1 \times d}$ ,  $\hat{\mathbf{E}}^i = \text{diag}\{s_1^i, \mathbf{E}_1^i, \dots, s_N^i, \mathbf{E}_N^i\}$  is the block diagonal matrix of  $s_j^i$  and Cholesky factorization  $\mathbf{E}_j^i, \mathbf{P}_j^i = \mathbf{E}_j^i(\mathbf{E}_j^i)^T$ ,  $\hat{\mathbf{e}}_m^{+,i} = \frac{D_{l_m}^{f,i} + U_{l_m}^{f,i}}{2}$ ,  $\hat{\mathbf{b}}_m^{+,i} = \frac{U_{l_m}^{f,i} - D_{l_m}^{f,i}}{2}$ ,  $l_m \in \mathcal{L}^{+,i}$ , as shown in (17),  $\mathbf{e}^{\varepsilon} = \frac{D^{\varepsilon} + U^{\varepsilon}}{2}$ ,  $\mathbf{b}^{\varepsilon} = \frac{U^{\varepsilon} - D^{\varepsilon}}{2}$  are shown in (2),  $(\Psi^{+, (i+1)})_{\perp}$  is the orthogonal complement of  $\Psi^{+, (i+1)}$  with full column rank, i.e., a basis of the null space of  $\Psi^{+, (i+1)}$ ,  $f^+ = [f_{l_1}, \dots, f_{l_{L^+}}]^T$ ,  $l_m \in \mathcal{L}^{+,i}$ ,  $m = 1, \dots, L^+$ ,  $\mathbf{J}^{+,i} = \frac{\partial f^+(x)}{\partial x}|_{\hat{\mathbf{x}}^i}$ ,  $L^+ = |\mathcal{L}^{+,i}|$ . The symbol  $\preceq$  is used to denote generalized inequality between symmetric matrices, it represents matrix inequality.

$$\begin{aligned} \Xi_n &= \text{diag}\left(1 - \sum_{j=1}^N \tau_j^1 - \sum_{j=1}^N \tau_j^2 - \sum_{l \in \mathcal{L}^{+,i}} \tau_l^+, \right. \\ &\quad \text{diag}(\tau_1^1, \tau_1^2, \dots, \tau_N^1, \tau_N^2 \mathbf{I}), \\ &\quad \left. \text{diag}(\tau_{l_1}^+, \dots, \tau_{l_{L^+}}^+)\right) + \sum_{l \in \mathcal{L}^{-,i}} \tau_l^- \Psi_l^{-, (i+1)}. \end{aligned} \quad (36)$$

(b) The state bounding set  $\mathcal{E}_n^{\rho, (i+1)}$ , as shown in (10), is obtained by solving the optimization problem in the

variables  $\mathbf{P}_n^{i+1}, \hat{\rho}_n^{i+1}$ , nonnegative scalars  $\tau_j^1 \geq 0, \tau_j^2 \geq 0, j = 1, \dots, N, \tau_l^+ \geq 0, l \in \mathcal{L}^{+,i}, \tau_l^- \geq 0, l \in \mathcal{L}^{-,i},$

$$\min g(\mathbf{P}_n^{i+1}) \quad (37)$$

subject to

$$\begin{aligned} -\tau_j^1 &\leq 0, -\tau_j^2 \leq 0, j = 1, \dots, N, \\ -\tau_l^+ &\leq 0, l \in \mathcal{L}^{+,i}, -\tau_l^- \leq 0, l \in \mathcal{L}^{-,i}, \end{aligned} \quad (38)$$

$$\begin{bmatrix} -\mathbf{P}_n^{i+1} \\ (\Phi_n^{\rho, (i+1)}(\Psi^{+, (i+1)})_{\perp}^T)_{\perp} \\ \Phi_2^{i+1}(\Psi^{+, (i+1)})_{\perp} \\ -(\Psi^{+, (i+1)})_{\perp}^T \Xi_n(\Psi^{+, (i+1)})_{\perp} \end{bmatrix} \preceq 0, \quad (39)$$

where

$$\Phi_n^{\rho, (i+1)} = [\hat{\rho}_n^i - \hat{\rho}_n^{i+1}, \mathbf{I}_n^2 \hat{\mathbf{E}}^i, 0, 0], \quad (40)$$

the  $n$ -th entry is  $\mathbf{I}_2$

$\mathbf{I}_n^2 = [0, \dots, \mathbf{I}_2, \dots, 0]$ ,  $\mathbf{I}_2 = [0 \ \mathbf{I}]$ ,  $\mathbf{0} \in \mathbb{R}^{d \times 1}$ ,  $\mathbf{I} \in \mathbb{R}^{d \times d}$  and other symbols are same as in problem (29)-(31).

**PROOF.** See the Appendix.

**Remark 7** In the problem (29)-(31),  $\mathcal{E}_n^{s, (i+1)}$  is estimated while  $\mathcal{E}_n^{\rho}$  and the parameter bounds of the other sources are fixed. In the problem (37)-(39),  $\mathcal{E}_n^{\rho, (i+1)}$  is estimated while  $\mathcal{E}_n^s$  and the parameter bounds of the other sources remain fixed. All the problems are feasible. Moreover,  $\mathcal{E}_n^{s, i}$  and  $\mathcal{E}_n^{\rho, i}$  are the feasible solutions of the two problems, respectively. The problem (29)-(31) is a convex SDP problem involving a constraint matrix of dimension  $M_1 = (d+1)N + L + 2$ , and  $M_2 = 2 + 2N + 2L$  decision variables. Therefore, using a general purpose primal-dual interior-point SDP solver, the practical complexity is  $O(M_1^2 M_2^2)$ . In our context, this corresponds to  $O(d^2)$  where  $d$  is the dimension of the state  $\rho$ ,  $O(N^4)$  where  $N$  is the number of sources, and  $O(L^4)$  where  $L$  is the number of sensors. In the same way, the complexity of the problem (37)-(39) corresponds to  $O(d^6)$  where  $d$  is the dimension of  $\rho$ ,  $O(N^4)$  where  $N$  is the number of sources, and  $O(L^4)$  where  $L$  is the number of sensors. Moreover, the decoupled technique in [9] can reduce the complexity when the dimension of the state is greater than one.

Using Propositions 1 and 4, we have the alternating optimization iterative algorithm, Algorithm 1, for the multiple-source localization problem. Moreover, the computational complexity of finding the remainder bound in Propositions 2 and 3 is greatly reduced compared to that of Proposition 1. In order to reduce the

---

**Algorithm 1** Ellipsoidal localization algorithm

---

**Require:**  $g(\mathbf{P})$ : objective function,  $\mathcal{E}_1^0 \times \dots \times \mathcal{E}_N^0$ : initial state bounding set,  $\mathcal{B}^\varepsilon$ : the bounding set of noises,  $\mathcal{B}_1^0 \times \dots \times \mathcal{B}_N^0$ : the bounding set of remainder,  $\delta > 0$ : tolerance.

- 1: **repeat**
- 2:   **Input:** the current state bound  $\prod_{n=1}^N \mathcal{E}_n^i$ , and the current remainder bound  $\prod_{n=1}^N \mathcal{B}_n^i$ .
- 3:   **for**  $n = 1, \dots, N$  **do**
  - (1) Optimize the center and shape matrix of the state bounding ellipsoid  $\mathcal{E}_n^{\rho, (i+1)}$  by the problem (37)-(39) in Proposition 4.
  - (2) Optimize the center and shape matrix of the state bounding ellipsoid  $\mathcal{E}_n^{s, (i+1)}$  by the problem (29)-(31) in Proposition 4.
  - (3) Derive the bounding set  $\mathcal{B}_n^{i+1}$ , by Proposition 1.
  - (4) **Update:** the current state bound  $\mathcal{E}_1^{i+1} \times \dots \times \mathcal{E}_n^{i+1} \times \mathcal{E}_{n+1}^i \times \dots \times \mathcal{E}_N^i$  and the current remainder bound  $\mathcal{B}_1^{i+1} \times \dots \times \mathcal{B}_n^{i+1} \times \mathcal{B}_{n+1}^i \times \dots \times \mathcal{B}_N^i$ .
- 4:   **end for**
- 5:   **Output:** the current state bound  $\mathcal{E}_1^{i+1} \times \dots \times \mathcal{E}_N^{i+1}$ , and the current remainder bound  $\mathcal{B}_1^{i+1} \times \dots \times \mathcal{B}_N^{i+1}$ .
- 6: **until**  $(g(\mathbf{P}^i) - g(\mathbf{P}^{i+1})) \leq \delta$

---

complexity, the ellipsoidal state bound  $\mathcal{E}^\rho$  is relaxed to a bounding ball where the radius is the long semi-axis of the ellipsoid  $\mathcal{E}^\rho$ . Thus, using Propositions 2-4, we can get the Algorithm 2.

**Remark 8** *Algorithm 1 and Algorithm 2 are similar to the block coordinate decent or nonlinear Gauss-Seidel methods. At each iteration, the objective function  $g(\mathbf{P}^{i+1})$  is minimized with respect to each of the “block coordinate” vectors  $\mathbf{x}_n$ , in a cyclic manner. The criterion for terminating the iterations is that the algorithm stops when the decrease of  $g(\mathbf{P}^{i+1})$  is sufficiently small, i.e.,  $g(\mathbf{P}^i) - g(\mathbf{P}^{i+1}) \leq \delta$ , where  $\delta$  is a small positive scalar. This method can converge to a stationary point. A detailed discussion of the method is found in [3], [48].*

**Remark 9** *When measurement data may contain outliers, the guaranteed outlier minimal number estimator (GOMNE) can be used to deal with the problem [19]. Moreover, gating is a screening technique that proves very effective in cutting down the number of unlikely tracks postulated for a target ([1], [2]). The idea of gating can also be used to delete outliers.*

## 5 $\alpha$ is unknown but bounded

In this section, we derive the multiple-source ellipsoidal localization method when  $\alpha$  is unknown but bounded. The main idea is that based on the separability of the nonlinear measurement function and interval mathematics, an efficient estimation procedure is developed to deal

---

**Algorithm 2** Simplified ellipsoidal localization algorithm

---

**Require:**  $g(\mathbf{P})$ : objective function,  $\mathcal{E}_1^0 \times \dots \times \mathcal{E}_N^0$ : initial state bounding set,  $\mathcal{B}^\varepsilon$ : the bounding set of noises,  $\mathcal{B}_1^0 \times \dots \times \mathcal{B}_N^0$ : the bounding set of remainder,  $\delta > 0$ : tolerance.

- 1: **repeat**
- 2:   **Input:** the current state bound  $\prod_{n=1}^N \mathcal{E}_n^i$ , and the current remainder bound  $\prod_{n=1}^N \mathcal{B}_n^i$ .
- 3:   **for**  $n = 1, \dots, N$  **do**
  - (1) Optimize the center and shape matrix of the state bounding ellipsoid  $\mathcal{E}_n^{\rho, (i+1)}$  by the problem (37)-(39) in Proposition 4.
  - (2) Optimize the center and shape matrix of the state bounding ellipsoid  $\mathcal{E}_n^{s, (i+1)}$  by the problem (29)-(31) in Proposition 4.
  - (3) Find the minimum ball which contains  $\mathcal{E}_n^{\rho, (i+1)}$ . Derive the bounding set  $\mathcal{B}_n^{i+1}$ , by Propositions 2 and 3.
  - (4) **Update:** the current state bound  $\mathcal{E}_1^{i+1} \times \dots \times \mathcal{E}_n^{i+1} \times \mathcal{E}_{n+1}^i \times \dots \times \mathcal{E}_N^i$  and the current remainder bound  $\mathcal{B}_1^{i+1} \times \dots \times \mathcal{B}_n^{i+1} \times \mathcal{B}_{n+1}^i \times \dots \times \mathcal{B}_N^i$ .
- 4:   **end for**
- 5:   **Output:** the current state bound  $\mathcal{E}_1^{i+1} \times \dots \times \mathcal{E}_N^{i+1}$ .
- 6: **until**  $(g(\mathbf{P}^i) - g(\mathbf{P}^{i+1})) \leq \delta$

---

with the multiple-source localization problem by using an alternating optimization iterative algorithm.

Consider the multiple source localization problem when  $\alpha$  is unknown but bounded. Since the decay factor  $\alpha$  usually lies between 2 to 4 (see [27]), we assume that  $\alpha$  is bounded and lies in  $[2, 4]$ , i.e.,  $\alpha \in [\alpha_1, \alpha_2] \subset [2, 4]$ . The measurement functions are written as

$$y_l = \sum_{n=1}^N f_{n,l}(\mathbf{x}_n) + \varepsilon_l, \quad l = 1, \dots, L, \quad (41)$$

where  $f_{n,l}(\mathbf{x}_n)$  is defined in (3). At the  $i$ -th iteration, the bounding set of the state  $\mathbf{x}$  is  $\mathcal{E}^i$ , which is defined in (10). The bounding interval  $[\check{D}_{n,l}^i, \check{U}_{n,l}^i]$  of the function  $f_{n,l}$  can be obtained.

**Lemma 5** *If the energy parameter and the position of the  $n$ -th source are bounded in  $\mathcal{E}_n^i$  which is defined in (10), and  $\alpha \in [\alpha_1, \alpha_2] \subset [2, 4]$ , then the bounding interval  $[\check{D}_{n,l}^i, \check{U}_{n,l}^i]$  of the function  $f_{n,l}$ , is obtained by solving the optimization problems*

$$D_{n,l}^\rho = \min \|\rho_n - r_l\| \quad (42)$$

*subject to*  $\rho_n \in \mathcal{E}_n^{\rho, i}$ ,

and

$$U_{n,l}^\rho = \max \|\rho_n - r_l\| \quad (43)$$

subject to  $\rho_n \in \mathcal{E}_n^{\rho,i}$ .

If  $D_{n,l}^\rho > 0$ ,

$$[\check{D}_{n,l}^i, \check{U}_{n,l}^i] = [g_l \frac{\hat{s}_n^i - S_n^i}{\max\{(U_{n,l}^\rho)^{\alpha_1}, (U_{n,l}^\rho)^{\alpha_2}\}}, g_l \frac{\hat{s}_n^i + S_n^i}{\min\{(D_{n,l}^\rho)^{\alpha_1}, (D_{n,l}^\rho)^{\alpha_2}\}}].$$

If  $D_{n,l}^\rho = 0$ ,

$$[\check{D}_{n,l}^i, \check{U}_{n,l}^i] = [g_l \frac{\hat{s}_n^i - S_n^i}{\max\{(U_{n,l}^\rho)^{\alpha_1}, (U_{n,l}^\rho)^{\alpha_2}\}}, +\infty],$$

where  $\hat{s}_n^i$  and  $S_n^i$  are defined in (10).

**PROOF.** See the Appendix.

**Remark 10** The optimization problem (42) is a second-order cone program (SOCP) and it can be solved by using Yalmip [20]. Using the S-procedure method, the optimization problem (43) is equivalent to the following optimization problem

$$\begin{aligned} & \min t \\ & \text{subject to } \tau \geq 0 \\ & \begin{bmatrix} \mathbf{I} & -r_l \\ -r_l^T & r_l^T r_l - t \end{bmatrix} \\ & -\tau \begin{bmatrix} (\mathbf{P}_n^i)^{-1} & -(\mathbf{P}_n^i)^{-1} \hat{\rho}_n^i \\ -((\mathbf{P}_n^i)^{-1} \hat{\rho}_n^i)^T & (\hat{\rho}_n^i)^T (\mathbf{P}_n^i)^{-1} \hat{\rho}_n^i - 1 \end{bmatrix} \preceq 0, \end{aligned} \quad (44)$$

where  $\mathbf{P}_n^i$  and  $\hat{\rho}_n^i$  are defined in (10).

We use the current state bound  $\mathcal{E}_1^i \times \dots \times \mathcal{E}_N^i$  and the bounding intervals  $[\check{D}_{n,l}^i, \check{U}_{n,l}^i]$  of the function  $f_{n,l}$ ,  $l = 1, \dots, L, n = 1, \dots, N$ , to determine the bounding set of the state at  $(i+1)$ -th iteration, i.e., look for  $\hat{\rho}_n^{i+1}$ ,  $\hat{s}_n^{i+1}$ ,  $S_n^{i+1}$  and  $\mathbf{P}_n^{i+1}$  of  $\mathcal{E}_n^{i+1}$  such that the state  $\mathbf{x}_n$  of the  $n$ -th source belongs to  $\mathcal{E}_n^{i+1}$ ,  $n = 1, \dots, N$ . It is obtained by the following proposition.

**Proposition 6** At  $(i+1)$ -th iteration, based on measurement  $\mathbf{y}$ , the current state bound  $\mathcal{E}_1^i \times \dots \times \mathcal{E}_N^i$ ,  $\alpha \in [\alpha_1, \alpha_2] \subset [2, 4]$ , the bounding interval  $[\check{D}_{n,l}^i, \check{U}_{n,l}^i]$  of the function  $f_{n,l}$ ,  $l = 1, \dots, L, n = 1, \dots, N$ , and the noise bounding box  $\mathcal{B}^\varepsilon$ , for the  $n$ -th source state  $\mathbf{x}_n$ ,  $n = 1, \dots, N$ , we have:

(a) The state bounding set  $\mathcal{E}_n^{\rho,(i+1)}$  as shown in (10), is obtained by solving the optimization problem in the variables  $\hat{\rho}_n^{i+1}$ ,  $\mathbf{P}_n^{i+1}$  and nonnegative scalars  $\tau^1 \geq 0$ ,  $\tau^2 \geq 0$ ,  $\tau_l^3 \geq 0$ ,  $l = 1, \dots, L$ ,  $\tau_l^4 \geq 0$ ,  $l \in \mathcal{L}^d$ ,

$$\min \text{trace}(\mathbf{P}_n^{i+1}) \quad (45)$$

subject to

$$\begin{aligned} & -\tau^1 \leq 0, -\tau^2 \leq 0, -\tau_l^3 \leq 0, l = 1, \dots, L, \\ & -\tau_l^4 \leq 0, l \in \mathcal{L}^d, \\ & \begin{bmatrix} -\mathbf{P}_n^{i+1} & \Psi_n^\rho \\ (\Psi_n^\rho)^T & -\Xi_n \end{bmatrix} \preceq 0, \end{aligned} \quad (46)$$

where

$$\begin{aligned} \Xi_n &= \text{diag}(1, 0, 0) + \tau^1 \Phi_n^\rho + \tau^2 \Phi_n^s \\ &+ \sum_{l=1}^L \tau_l^3 \Phi_{n,l}^u + \sum_{l \in \mathcal{L}^d} \tau_l^4 \Phi_{n,l}^d, \end{aligned} \quad (47)$$

$$\Phi_{n,l}^u = - \begin{bmatrix} r_l^T r_l & -\frac{1}{2\check{U}_{n,l}} & -r_l^T \\ -\frac{1}{2\check{U}_{n,l}} & 0 & \mathbf{0} \\ -r_l & \mathbf{0} & \mathbf{I} \end{bmatrix}, \quad (48)$$

$$\Phi_{n,l}^d = \begin{bmatrix} r_l^T r_l & -\frac{1}{2\check{D}_{n,l}} & -r_l^T \\ -\frac{1}{2\check{D}_{n,l}} & 0 & \mathbf{0} \\ -r_l & \mathbf{0} & \mathbf{I} \end{bmatrix}, \quad (49)$$

$$\Phi_n^\rho = \begin{bmatrix} (\hat{\rho}_n^i)^T (\mathbf{P}_n^i)^{-1} \hat{\rho}_n^i - 1 & \mathbf{0} & -(\hat{\rho}_n^i)^T (\mathbf{P}_n^i)^{-1} \\ \mathbf{0} & \mathbf{0} & \mathbf{0} \\ -((\hat{\rho}_n^i)^T (\mathbf{P}_n^i)^{-1}) & \mathbf{0} & (\mathbf{P}_n^i)^{-1} \end{bmatrix}, \quad (50)$$

$$\Phi_n^s = \begin{bmatrix} D_n^s U_n^s & -\frac{D_n^s + U_n^s}{2} & \mathbf{0} \\ -\frac{D_n^s + U_n^s}{2} & 1 & \mathbf{0} \\ \mathbf{0} & \mathbf{0} & \mathbf{0} \end{bmatrix}, \quad (51)$$

$$\Psi_n^\rho = \begin{bmatrix} -\hat{\rho}_n^{i+1} & \mathbf{0} & \mathbf{I} \end{bmatrix}. \quad (52)$$

$$\begin{aligned} D_n^s &= \min\{(\hat{s}_n^i - S_n^i)^{2/\alpha_1}, (\hat{s}_n^i - S_n^i)^{2/\alpha_2}\}, U_n^s = \\ & \max\{(\hat{s}_n^i + S_n^i)^{2/\alpha_1}, (\hat{s}_n^i + S_n^i)^{2/\alpha_2}\}, \\ \tilde{D}_{n,l} &= \min\{(\max\{\frac{y_l - \check{U}_{n,l}^i}{g_l}, 0\})^{2/\alpha_1}, (\max\{\frac{y_l - \check{U}_{n,l}^i}{g_l}, 0\})^{2/\alpha_2}\}, \\ \tilde{U}_{n,l} &= \min\{(\frac{y_l - \hat{D}_{n,l}^i}{g_l})^{2/\alpha_1}, (\frac{y_l - \hat{D}_{n,l}^i}{g_l})^{2/\alpha_2}\}, \hat{D}_{n,l} = \\ & \sum_{j \neq n} \check{D}_{l,j} + \mathbf{D}_l^\varepsilon, \text{ and } \hat{U}_{n,l} = \sum_{j \neq n} \check{U}_{l,j} + \mathbf{U}_l^\varepsilon. \end{aligned}$$

$$\mathcal{L}^d = \{l : \tilde{D}_{n,l} > 0, l = 1, \dots, L\}. \quad (53)$$

(b) The state bounding set  $\mathcal{E}_n^{s,(i+1)}$  as shown in (10), is obtained by solving the optimization problem in the

variables  $\tilde{s}_n, \tilde{S}_n$  and nonnegative scalars  $\tau^1 \geq 0, \tau^2 \geq 0, \tau_l^3 \geq 0, l = 1, \dots, L, \tau_l^4 \geq 0, l \in \mathcal{L}^d$ ,

$$\min \tilde{S}_n \quad (54)$$

subject to

$$\begin{aligned} -\tau^1 &\leq 0, -\tau^2 \leq 0, -\tau_l^3 \leq 0, l = 1, \dots, L, \\ -\tau_l^4 &\leq 0, l \in \mathcal{L}^d, \\ \begin{bmatrix} -\tilde{S}_n & \Psi_n^s \\ (\Psi_n^s)^T & -\Xi_n \end{bmatrix} &\preceq 0, \end{aligned} \quad (55)$$

where  $\Psi_n^s = \begin{bmatrix} -\tilde{S}_n & \mathbf{1} & \mathbf{0} \end{bmatrix}$ , and other symbols are same as in (a).

We can obtain

$$\hat{S}_n^{i+1} = \frac{U_s + D_s}{2}, \quad s_n^{i+1} = \frac{U_s - D_s}{2},$$

where  $D_s = \min\{(\tilde{s}_n^* - \tilde{S}_n^*)^{\alpha_1/2}, (\tilde{s}_n^* - \tilde{S}_n^*)^{\alpha_2/2}\}$ ,  $U_s = \max\{(\tilde{s}_n^* + \tilde{S}_n^*)^{\alpha_1/2}, (\tilde{s}_n^* + \tilde{S}_n^*)^{\alpha_2/2}\}$  and  $\tilde{s}_n^*, \tilde{S}_n^*$  are the optimal solution of the problem (54)-(55).

**PROOF.** See the Appendix.

Using Lemma 5 and Proposition 6, we have the alternating optimization iterative algorithm, Algorithm 3, for the multiple-source localization problem with unknown but bounded  $\alpha$ .

**Algorithm 3** Ellipsoidal localization algorithm with unknown but bounded  $\alpha$

**Require:**  $g(\mathbf{P})$ : objective function,  $\mathcal{E}_1^0 \times \dots \times \mathcal{E}_N^0$ : initial state bounding set,  $\mathcal{B}^\varepsilon$ : the bounding,  $\delta > 0$ : tolerance.

1: **repeat**

2:   **Input:** the current state bound  $\prod_{n=1}^N \mathcal{E}_n^i$ .

3:   Derive the bounding intervals  $[\hat{D}_{n,l}^i, \hat{U}_{n,l}^i]$ ,  $l = 1, \dots, L, n = 1, \dots, N$ , by Lemma 5.

4:   **for**  $n = 1, \dots, N$  **do**

(1) Optimize the center and shape matrix of the state bounding ellipsoid  $\mathcal{E}_n^{\rho, (i+1)}$  by the problem (45)-(46) in Proposition 6.

(2) Optimize the center and shape matrix of the state bounding ellipsoid  $\mathcal{E}_n^{s, (i+1)}$  by the problem (54)-(55) in Proposition 6.

5:   **end for**

6:   **Output:** the current state bound  $\mathcal{E}_1^{i+1} \times \dots \times \mathcal{E}_N^{i+1}$ .

7: **until**  $(g(\mathbf{P}^i) - g(\mathbf{P}^{i+1})) \leq \delta$

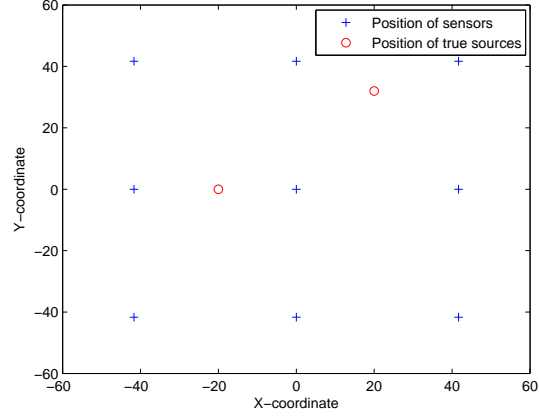


Fig. 2. The positions of two sources and the sensors placed on a grid.

## 6 Simulation Results

In this section, we compare the performances of Algorithm 1 (Alg-1) and Algorithm 2 (Alg-2) with that of the EM method in [27]. For performance comparison, we employ the Mean Squared Error (MSE) based on 200 Monte Carlo runs. The size of the sensor field is  $100m \times 100m$ .

We use the measurement equation (1) to generate the acoustic energy reading for each sensor. The gain factors for all the sensors are equal to 1 and the decay factor  $\alpha = 2$ . The measurement noises are independent random variables with truncated Gaussian mixture distribution, i.e.,  $\varepsilon_l \sim h_l(x) = c(\frac{1}{2}h_{l,1}(x) + \frac{1}{2}h_{l,2}(x))I_{[-\frac{b_l^\varepsilon}{2}, \frac{b_l^\varepsilon}{2}]}(x)$ , where  $b^\varepsilon = \frac{U^\varepsilon - D^\varepsilon}{2}$  is the vector of the side lengths of the bounding box of the measurement noise,  $U^\varepsilon$  and  $D^\varepsilon$  are defined in (2).  $h_{l,i} \sim \mathcal{N}(\mu_i, \sigma_i^2)$ ,  $i = 1, 2$ ,  $\mu_1 = \frac{b_1^\varepsilon}{2}$ ,  $\sigma_1 = \frac{b_1^\varepsilon}{6}$ ,  $\mu_2 = -\frac{b_1^\varepsilon}{2}$ ,  $\sigma_2 = \frac{b_1^\varepsilon}{6}$ ,  $c$  is the normalizing constant, and  $I_{[-\frac{b_l^\varepsilon}{2}, \frac{b_l^\varepsilon}{2}]}(x)$  is an indicator function of the set  $[-\frac{b_l^\varepsilon}{2}, \frac{b_l^\varepsilon}{2}]$ . Moreover, set all the components of the vector  $b^\varepsilon$  to be equal.

Nine sensor nodes are placed on a regular grid as shown in Fig. 2. The sensor locations remain fixed during all the Monte Carlo runs. Two acoustic sources are located at  $[-20, 0]$  and  $[20, 32]$ , respectively. The source energies are assumed to be  $s_1 = 6000$ , and  $s_2 = 6500$ . The initial state bounding set is  $\mathcal{E}^0$ , shown in (9). For the  $n$ -th source,  $n = 1, 2$ , the Cartesian product of ellipsoids  $\mathcal{E}_n^0 = \mathcal{E}_n^{s,0} \times \mathcal{E}_n^{\rho,0}$  is randomly selected in each run, where  $\mathcal{E}_n^{s,0}$  is an interval of length 200 and  $\mathcal{E}_n^{\rho,0}$  is a ball of radius  $7m$ . The MSEs of Alg-1, Alg-2 and the EM method are plotted as a function of  $b^\varepsilon$  in Fig. 3, respectively. To further understand the simplified Algorithm 2, we have presented additional numerical simulations, see Fig. 6- Fig. 8. The state estimates of the two sources are plotted as a function of the number of iterations, number of sensors and distance between two sources, respectively.

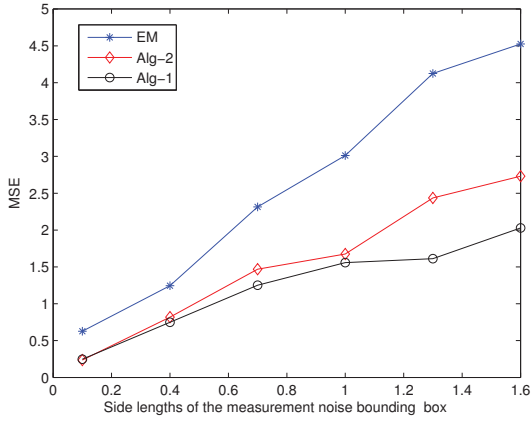


Fig. 3. MSE of the state estimates for two sources and sensor locations are shown in Fig. 2 is plotted as a function of  $b^\epsilon$ .

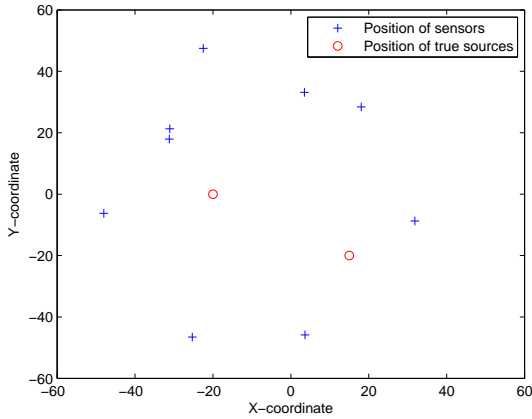


Fig. 4. The positions of the sources and the sensors when sensors are located randomly in the region of interest.

Moreover, we also consider a scenario in which sensor node locations are not on a grid and are random as shown in Fig. 4. Two acoustic sources are located at  $[-20, 0]$  and  $[15, -20]$ , respectively. The MSEs of Alg-1, Alg-2 and the EM method are plotted as a function of  $b_\epsilon$  in Fig. 5, respectively.

Similarly, the localization problem for three sensors is considered next. Sensor nodes are placed as shown in Fig.9 and Fig.11, respectively. As shown in Fig.9, three acoustic sources are located at  $[-20, 0]$ ,  $[20, 32]$  and  $[20, -20]$ , respectively. The source energies are  $s_1 = 6000$ ,  $s_2 = 6500$  and  $s_3 = 6800$  respectively. The MSEs of Alg-1, Alg-2 and the EM method are plotted as a function of  $b_\epsilon$  in Fig. 10. The locations of all the sensors in Fig.11 are random. Three acoustic sources are located at  $[-25, 0]$ ,  $[15, 19]$  and  $[20, -15]$ , respectively. The MSEs of Alg-1, Alg-2 and the EM method are plotted as a function of  $b^\epsilon$  in Fig. 12. The computation times of the three algorithms are shown in Table 1. The time in each case is the mean of 200 Monte Carlo runs.

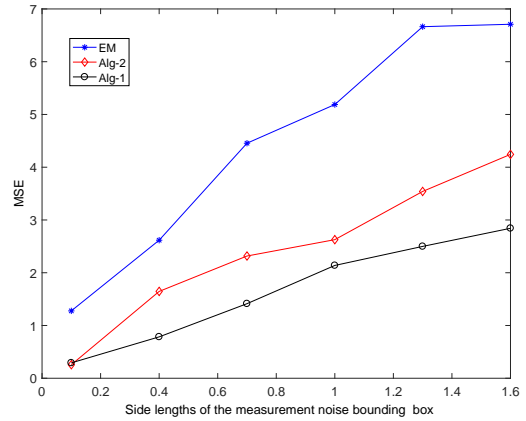


Fig. 5. MSE of the state estimates for two sources for randomly located sensors as shown in Fig. 4 is plotted as a function of  $b^\epsilon$ .

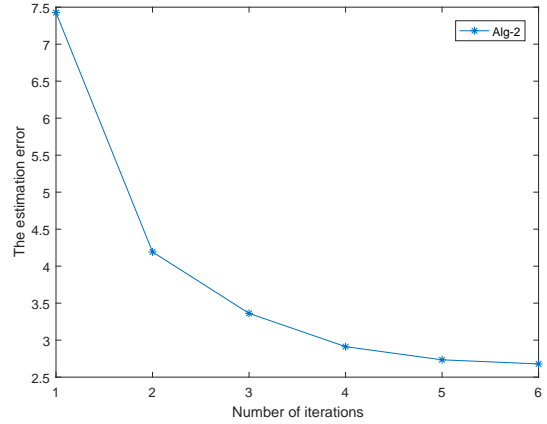


Fig. 6. The state estimation error for two sources is plotted as a function of the number of iterations.

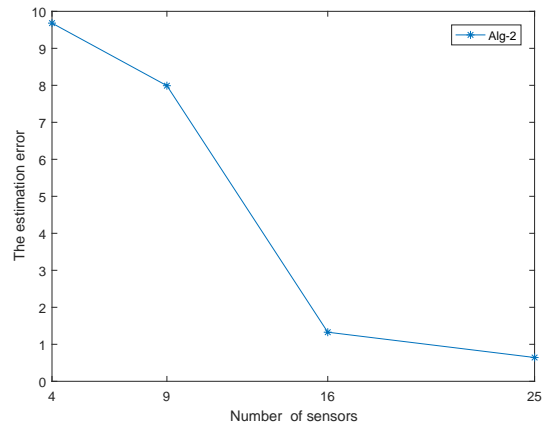


Fig. 7. The state estimation error for two sources is plotted as a function of the number of sensors.

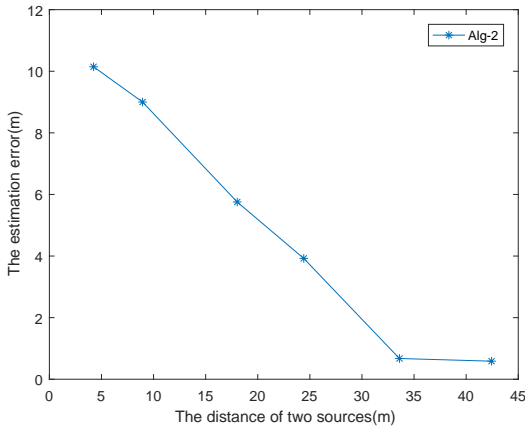


Fig. 8. The state estimation error for two sources is plotted as a function of the distance between two sources.

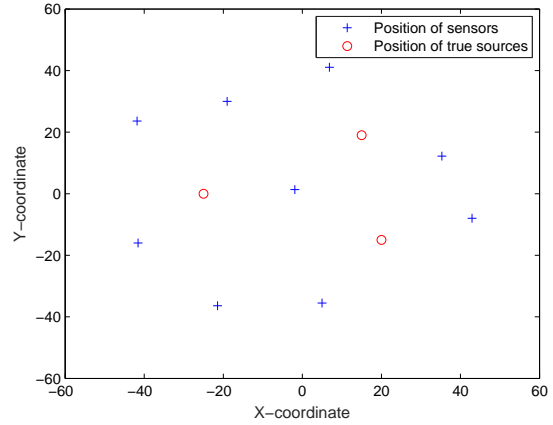


Fig. 11. The positions of three sources and the sensors placed randomly in the region of interest.

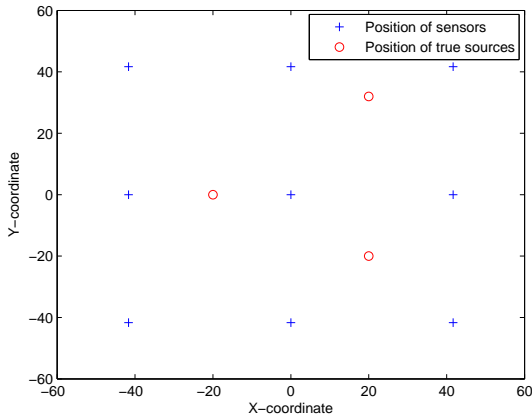


Fig. 9. The positions of three sources and the sensors placed on a grid.

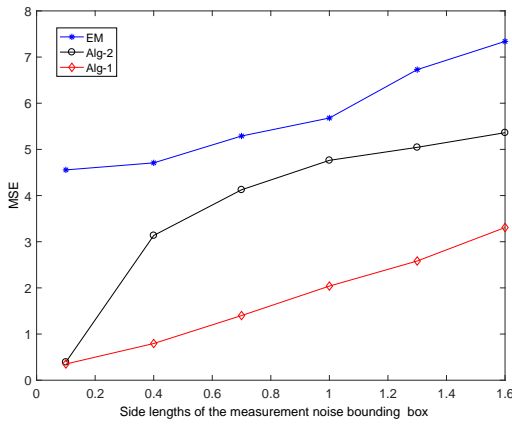


Fig. 10. MSE of the state estimates for three sources with sensors located on a grid as shown in Fig. 9 is plotted as a function of  $b^\varepsilon$ .

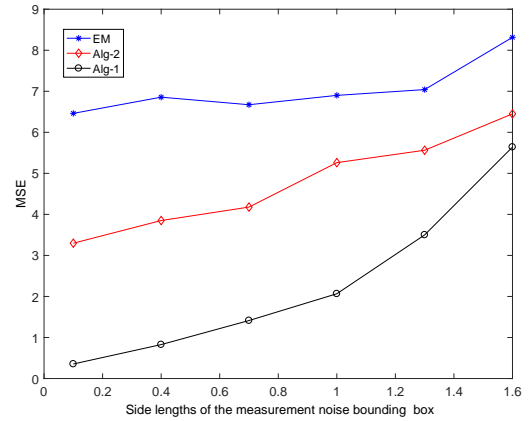


Fig. 12. MSE of the state estimates for three sources with sensors located as shown in Fig. 11 is plotted as a function of  $b^\varepsilon$ .

Table 1  
The Computation Time of Different Algorithms

time(s) \ method	EM	Alg-1	Alg-2
Source			
two sources	3.03	46.3	24.03
three sources	16.8	76.6	52.2

When the energy decay factor  $\alpha$  is unknown but bounded, i.e.,  $\alpha \in [2.8, 3.2]$ , the estimation error of Algorithm 3 (Alg-3) is shown in Fig. 13 where there are two sources and 16 sensors. It is plotted as a function of the number of iterations.

From Figs. 2-13, we make the following observations:

- Figs. 2-4 and Figs. 9-12 show that the performances of both Alg-1 and Alg-2 are better than that of the EM method. The main reason is that the EM method is

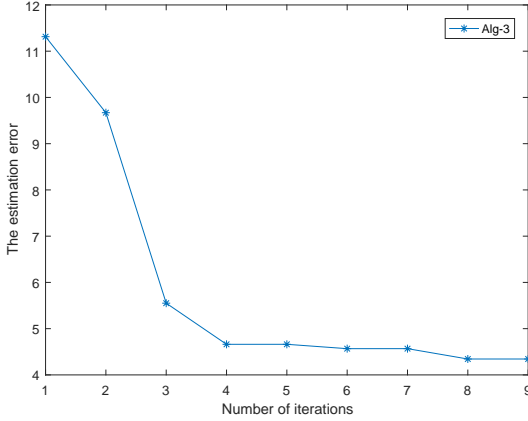


Fig. 13. The state estimation error for two sources when  $\alpha$  is unknown but bounded, is plotted as a function of the number of iterations.

based on the Gaussian assumption. However, in this example, the measurement noise is non-Gaussian. Actually, the ellipsoidal localization approach presented in this paper in the unknown but bounded setting only depends on the bounds of noises and does not rely on the probability density function (PDF). In addition, the figures show that the larger is the noise bound  $b^\varepsilon$ , the larger is the MSE.

- Figs. 2-4 and Figs. 9-12 also show that the performance of Alg-1 is better than that of Alg-2 since the ellipsoidal state bound  $\mathcal{E}^\rho$  in Proposition 1 is relaxed to a bounding ball in Proposition 2 where the radius is the long semi-axis of the ellipsoid  $\mathcal{E}^\rho$ . However, Alg-2 requires less computation time than Alg-1, as shown in Table 1. The reason is that the solution of the remainder bound is obtained by solving an SDP problem in Proposition 1 whereas the bounding box of the remainder is obtained analytically in Proposition 2. Thus, there is a tradeoff between computation time and localization accuracy.
- The estimation error of Alg-2 is plotted as a function of the number of iterations in Fig. 6. It shows that the performance improves with the number of iterations and then it becomes stable. Fig. 7 shows that the estimation improves with the number of sensors. Fig. 8 shows that the distance between the sources affects the localization accuracy. If sources are too close, the accuracy decreases. With an increase of source spacing, the localization accuracy becomes better. Fig. 13 shows that Alg-3 can deal with the multiple source localization problem when  $\alpha$  is unknown but bounded. The estimation error decreases with the number of iterations.
- As shown in Figs. 6 and 13, the estimation accuracy improves slowly after several iterations. The estimation accuracy increases with the decrease of  $\delta$ , but the computation time increases at the same time. For the trade-off between the computation time and the estimation accuracy, a reasonable value for the termina-

tion criterion might be  $\delta = 10^{-2}$ . Furthermore, the numerical simulation also shows that the size of the final shape matrix becomes stable with the number of iterations. When the value of  $\delta$  is smaller than  $10^{-2}$ , the size of the final shape matrix does not change much.

- In summary, numerical examples show that when the PDF of measurement noise is unknown-but-bounded, Alg-1 is most effective for multiple-source localization as far as the estimation performance is considered. The computation time of the EM algorithm is the smallest. Alg-2 provides a good trade off between estimation performance and computation time.

## 7 Conclusion

In this paper, we have proposed new multiple-source localization methods in the unknown-but-bounded noise setting. We employed set-membership estimation theory to determine a state estimation ellipsoid. The main difficulties are that the acoustic energy decay model is a complicated nonlinear function and the multiple-source localization problem is a high-dimensional state estimation problem. In our approach, the nonlinear function is linearized by the first-order Taylor series expansion with a remainder error. The bounding box of the remainder has been derived on-line based on the bounding set of the state. A point that should be stressed is that the remainder bounding box is obtained analytically when the energy parameter and the position of the source are bounded in an interval and a ball respectively. An efficient procedure has been developed to deal with the multiple-source localization problem by alternately estimating the parameters of each source while the parameters of the other sources remain fixed. When the energy decay factor is unknown but bounded, a new estimation procedure has been developed. Numerical examples have shown that when the PDF of measurement noise is non-Gaussian, the performance of the ellipsoidal localization algorithm is better than the ML method. Future work may include sensor management and sensor placement, Byzantines and mitigation techniques, for the multiple-source localization problem in wireless sensor networks.

## A Proof of Proposition 1

Let  $\mathbf{x}_n = \hat{\mathbf{x}}_n^i + [\Delta s, \Delta \rho^T]^T$ , the function  $\Delta f_{n,l}(\mathbf{x}_n, \hat{\mathbf{x}}_n^i)$  is rewritten as

$$\Delta \tilde{f}_{n,l}(\Delta \rho, \Delta s) = g_l \left( \frac{\hat{s}_n^i + \Delta s}{\|\hat{\rho}_n^i - r_l + \Delta \rho\|^\alpha} - \frac{\hat{s}_n^i + \Delta s}{\|\hat{\rho}_n^i - r_l\|^\alpha} + \alpha \hat{s}_n^i \frac{(\hat{\rho}_n^i - r_l)^T}{\|\hat{\rho}_n^i - r_l\|^{\alpha+2}} \Delta \rho \right). \quad (\text{A.1})$$

The derived functions of  $\Delta \tilde{f}_{n,l}$  are

$$\begin{aligned} \frac{\partial \Delta \tilde{f}_{n,l}(\Delta \rho, \Delta s)}{\partial \Delta \rho} &= g_l \left( \frac{\alpha \hat{s}_n^i}{\|\hat{\rho}_n^i - r_l\|^{\alpha+2}} (\hat{\rho}_n^i - r_l) \right. \\ &\quad \left. - \frac{\alpha (\hat{s}_n^i + \Delta s)}{\|\hat{\rho}_n^i - r_l + \Delta \rho\|^{\alpha+2}} (\hat{\rho}_n^i - r_l + \Delta \rho) \right), \\ \frac{\partial \Delta \tilde{f}_{n,l}(\Delta \rho, \Delta s)}{\partial \Delta s} &= g_l \left( \frac{1}{\|\hat{\rho}_n^i - r_l + \Delta \rho\|^\alpha} \right. \\ &\quad \left. - \frac{1}{\|\hat{\rho}_n^i - r_l\|^\alpha} \right). \end{aligned}$$

If  $[\Delta s, \Delta \rho^T]^T$  is a stationary point, then

$$\frac{\partial \Delta \tilde{f}_{n,l}(\Delta \rho, \Delta s)}{\partial \Delta \rho} = 0, \quad \frac{\partial \Delta \tilde{f}_{n,l}(\Delta \rho, \Delta s)}{\partial \Delta s} = 0.$$

We can get

$$\begin{aligned} \frac{|\hat{s}_n^i + \Delta s|}{\hat{s}_n^i} \|\hat{\rho}_n^i - r_l + \Delta \rho\| &= \|\hat{\rho}_n^i - r_l\|, \\ \|\hat{\rho}_n^i - r_l + \Delta \rho\| &= \|\hat{\rho}_n^i - r_l\|, \end{aligned}$$

where  $\|\hat{\rho}_n^i - r_l\| > 0$ ,  $\hat{s}_n^i + \Delta s > 0$ , then  $\Delta s = 0$  and  $\Delta \rho = 0$ . It means that there is only one stationary point in  $\mathcal{E}_n^i$  and it is  $\hat{\mathbf{x}}_n^i = [\hat{s}_n^i, (\hat{\rho}_n^i)^T]^T$ .

If the  $l$ -th sensor is not contained in the set  $\mathcal{E}_n^{\rho,i}$ , then the function  $\Delta f_{n,l}(\mathbf{x}_n, \hat{\mathbf{x}}_n^i)$  is differentiable on the set  $\mathcal{E}_n^i$ . Since there is only one stationary point in  $\mathcal{E}_n^i$ , the minimum and maximum of  $\Delta f_{n,l}(\mathbf{x}_n, \hat{\mathbf{x}}_n^i)$  are obtained at the stationary point  $\hat{\mathbf{x}}_n^i$  or on the boundary of  $\mathcal{E}_n^i$ .

If the  $l$ -th sensor is contained in the set  $\mathcal{E}_n^{\rho,i}$ , for the same reason, then the minimum of  $\Delta f_{n,l}(\mathbf{x}_n, \hat{\mathbf{x}}_n^i)$  is obtained at the stationary point  $\hat{\mathbf{x}}_n^i$  or on the boundary of  $\mathcal{E}_n^i$ . The maximum of  $\Delta f_{n,l}(\mathbf{x}_n, \hat{\mathbf{x}}_n^i)$  is  $+\infty$  and it is obtained at  $\Delta \rho = -(\hat{\rho}_n^i - r_l)$ .

Therefore, we have Proposition 1.  $\square$

## B Proof of Proposition 2

For  $l = 1, \dots, L$ ,  $\Delta \tilde{f}_{n,l}(\Delta \rho, \Delta s)$  is defined (A.1). Since  $g_l$  is a positive constant, we only consider the following function

$$H(\Delta \rho, \Delta s) = \frac{\Delta \tilde{f}_{n,l}(\Delta \rho, \Delta s)}{g_l}. \quad (\text{B.1})$$

Let  $\tau_l = \|\hat{\rho}_n^i - r_l\|$ ,  $t = \|\Delta \rho\| \in [0, R_n^i]$ ,  $k = \cos(\theta)$  and  $\theta \in [0, \pi]$ , so that we can rewrite (B.1) as

$$H(k, \Delta s, t) = \frac{\hat{s}_n^i + \Delta s}{(t^2 + \tau_l^2 + 2t\tau_l k)^{\alpha/2}} + \frac{\alpha \hat{s}_n^i t k}{\tau_l^{\alpha+1}} - \frac{\hat{s}_n^i + \Delta s}{\tau_l^\alpha},$$

where  $k \in [-1, 1]$ ,  $\Delta s \in [-S_n^i, S_n^i]$ ,  $t \in [0, R_n^i]$ , and  $R_n^i < \tau_l$ .

The proof falls naturally into two parts: (I) find the maximum of the function  $H(k, \Delta s, t)$  when  $k \in [-1, 1]$ ,  $\Delta s \in [-S_n^i, S_n^i]$ ,  $t \in [0, R_n^i]$ , (II) find the minimum of the function  $H(k, \Delta s, t)$  when  $k \in [-1, 1]$ ,  $\Delta s \in [-S_n^i, S_n^i]$ ,  $t \in [0, R_n^i]$ .

(I) It is clear that  $H(k, \Delta s, t)$  is a linear function of  $\Delta s$ . Moreover, by Proposition 1, in order to get the maximum of the function  $H(k, \Delta s, t)$  on  $k$  and  $t$ , we only need to consider the two cases: (i)  $k \in [-1, 1]$ ,  $\Delta s = -S_n^i$ ,  $t \in [0, R_n^i]$ , (ii)  $k \in [-1, 1]$ ,  $\Delta s = S_n^i$ ,  $t \in [0, R_n^i]$ .

(i) Since  $H(k, -S_n^i, t)$  is a convex function of  $k$ , the maximum is obtained at  $k = 1$  or  $-1$ . It means that we only need to consider two functions of  $t$ :  $H(1, -S_n^i, t)$  and  $H(-1, -S_n^i, t)$ .

Since  $H(1, -S_n^i, t)$  is a convex function of  $t$ , the maximum is obtained at  $t = 0$  or  $R_n^i$ . It is easily seen that  $H(1, -S_n^i, 0) = 0$ . We get

$$\max_{t \in [0, R_n^i]} H(1, -S_n^i, t) = \max\{H(1, -S_n^i, R_n^i), 0\}. \quad (\text{B.2})$$

In the same manner we can see that

$$\max_{t \in [0, R_n^i]} H(-1, -S_n^i, t) = \max\{H(-1, -S_n^i, R_n^i), 0\}. \quad (\text{B.3})$$

(ii) For  $H(k, S_n^i, t)$  is a convex function of  $k$ , the maximum is obtained at  $k = 1$  or  $-1$ . It means that we only need to consider two functions of  $t$ :  $H(1, S_n^i, t)$  and  $H(-1, S_n^i, t)$ .

It is obvious that  $H(1, \Delta s, t)$  is a monotonic decreasing function of  $\Delta s$ . We have  $H(1, S_n^i, t) \leq H(1, -S_n^i, t)$  and

$$\max_{t \in [0, R_n^i]} H(1, S_n^i, t) \leq \max_{t \in [0, R_n^i]} H(1, -S_n^i, t). \quad (\text{B.4})$$

Since  $H(-1, S_n^i, t)$  is a convex function of  $t$ , the maximum is obtained at  $t = 0$  or  $R_n^i$ . We have  $H(-1, S_n^i, 0) = 0$  and

$$\max_{t \in [0, R_n^i]} H(-1, S_n^i, t) = \max\{H(-1, S_n^i, R_n^i), 0\}. \quad (\text{B.5})$$

Combining (B.2), (B.3), (B.4) and (B.5), we conclude that

$$\begin{aligned} &\max_{k \in [-1, 1], \Delta s \in [-S_n^i, S_n^i], t \in [0, R_n^i]} H(k, \Delta s, t) \\ &= \max\{H(1, -S_n^i, R_n^i), H(-1, S_n^i, R_n^i), \\ &\quad H(-1, -S_n^i, R_n^i), 0\}. \end{aligned} \quad (\text{B.6})$$

(II) Similar arguments apply to this case, in order to get the minimum of the function  $H(k, \Delta s, t)$  on  $k$  and  $t$ , we only need to consider the two cases: (i)  $k \in [-1, 1]$ ,  $\Delta s = -S_n^i$ ,  $t \in [0, R_n^i]$ , (ii)  $k \in [-1, 1]$ ,  $\Delta s = S_n^i$ ,  $t \in [0, R_n^i]$ .

(i) Let  $\frac{\partial H(k, -S_n^i, t)}{\partial k} = 0$ , we have

$$\hat{k}_1 = \frac{\left( \left(1 - \frac{S_n^i}{\hat{s}_n^i}\right)^{1/(\alpha/2+1)} - 1 \right) \tau_l^2 - t^2}{2t\tau_l} \leq 0. \quad (\text{B.7})$$

Since  $H(k, -S_n^i, t)$  is a convex function of  $k$ , the minimum is obtained at  $k = \hat{k}_1$  when  $\hat{k}_1 \in [-1, 1]$ . If  $\hat{k}_1 \notin [-1, 1]$ , the minimum is obtained at  $k = -1$  when  $\hat{k}_1 \notin [-1, 1]$ .

Let  $\frac{\partial H(-1, -S_n^i, t)}{\partial t} = 0$ , we get

$$t = \tau \left( 1 - \left(1 - \frac{S_n^i}{\hat{s}_n^i}\right)^{1/(\alpha+1)} \right) \geq 0.$$

Since  $H(-1, -S_n^i, t)$  is a convex function of  $t$ , we obtain

$$\min_{t \in [0, R_n^i]} H(-1, -S_n^i, t) = H(-1, -S_n^i, t_1). \quad (\text{B.8})$$

where  $t_1$  is defined in (22).

Consider the function

$$H(\hat{k}, -S_n^i, t) = \hat{s}_n^i \left( \frac{2 \left(1 - \frac{S_n^i}{\hat{s}_n^i}\right)^{1/(\alpha/2+1)} - 1 - \left(1 - \frac{S_n^i}{\hat{s}_n^i}\right)}{\tau_l^\alpha} - \frac{t^2}{\tau_l^{\alpha+2}} \right),$$

where  $\hat{k}_1 \in [-1, 1]$ . It is equivalent to

$$\left| \left(1 - \frac{S_n^i}{\hat{s}_n^i}\right)^{1/(\alpha+2)} - 1 \right| \tau_l \leq t. \quad (\text{B.9})$$

In this case, the minimum is  $H(\hat{k}_1, -S_n^i, R_n^i)$ .

Now we have

$$\begin{aligned} & \min_{k \in [-1, 1], t \in [0, R_n^i]} H(k, -S_n^i, R_n^i) \\ & = \min\{H(-1, -S_n^i, t_1), H(\max\{\hat{k}_1, -1\}, -S_n^i, R_n^i)\}. \end{aligned} \quad (\text{B.10})$$

(ii) Let  $\frac{\partial H(k, S_n^i, t)}{\partial k} = 0$ , we have

$$\hat{k}_2 = \frac{\left( \left(1 + \frac{S_n^i}{\hat{s}_n^i}\right)^{1/(\alpha/2+1)} - 1 \right) \tau_l^2 - t^2}{2t\tau_l}. \quad (\text{B.11})$$

Since  $H(k, S_n^i, t)$  is a convex function of  $k$ , the minimum is obtained at  $k = \hat{k}_2$  when  $\hat{k}_2 \in [-1, 1]$  and the minimum is obtained at  $k = 1$  or  $-1$  when  $\hat{k}_2 \notin [-1, 1]$ .

Let  $\frac{\partial H(1, S_n^i, t)}{\partial t} = 0$ , we get  $t = \tau \left( \left(1 + \frac{S_n^i}{\hat{s}_n^i}\right)^{1/(\alpha+1)} - 1 \right) > 0$ . Since  $H(1, S_n^i, t)$  is a convex function of  $t$ , we have

$$\min_{t \in [0, R_n^i]} H(1, S_n^i, t) = H(1, S_n^i, t_2), \quad (\text{B.12})$$

where  $t_2$  is defined in (23).

Let  $\frac{\partial H(-1, S_n^i, t)}{\partial t} = 0$ , we get

$$t = \tau \left( 1 - \left(1 + \frac{S_n^i}{\hat{s}_n^i}\right)^{1/(\alpha+1)} \right) \leq 0.$$

Since  $H(-1, s, t)$  is a convex function of  $t$ , we obtain

$$\min_{t \in [0, R_n^i]} H(-1, S_n^i, t) = 0. \quad (\text{B.13})$$

Consider the function

$$H(\hat{k}_2, S_n^i, t) = \hat{s}_n^i \left( \frac{2 \left(1 + \frac{S_n^i}{\hat{s}_n^i}\right)^{1/(\alpha/2+1)} - 1 - \left(1 + \frac{S_n^i}{\hat{s}_n^i}\right)}{\tau_l^\alpha} - \frac{t^2}{\tau_l^{\alpha+2}} \right),$$

where  $\hat{k}_2 \in [-1, 1]$ . It is equivalent to

$$\left| \left(1 + \frac{S_n^i}{\hat{s}_n^i}\right)^{1/(\alpha+2)} - 1 \right| \tau_l \leq t. \quad (\text{B.14})$$

In this case, the minimum is  $H(\hat{k}_2, S_n^i, R_n^i)$ .

Now we have

$$\begin{aligned} & \min_{k \in [-1, 1], t \in [0, R_n^i]} H(k, S_n^i, R_n^i) \\ & = \min\{H(\max\{-1, \min\{\hat{k}_1, 1\}\}, S_n^i, R_n^i), 0, \\ & \quad H(1, S_n^i, t_2)\}. \end{aligned} \quad (\text{B.15})$$

Therefore, from (B.10) and (B.15), we have the following result

$$\begin{aligned} & \min_{k \in [-1, 1], \Delta s \in [-S_n^i, S_n^i], t \in [0, R_n^i]} H(k, \Delta s, t) \\ & = \min\{H(-1, -S_n^i, t_1), H(\max\{\hat{k}_1, -1\}, -S_n^i, R_n^i), \\ & \quad H(1, S_n^i, t_2), 0, H(\max\{-1, \min\{\hat{k}_1, 1\}\}, S_n^i, R_n^i)\}. \end{aligned} \quad (\text{B.16})$$

Base on Equations (B.1), (B.6) and (B.16), we have actually proved the Proposition 2.  $\square$

### C Proof of Proposition 3

All symbols are same as those in the proof of Proposition 2. The proof is divided into two parts: (I) find the minimum of the function  $H(k, \Delta s, t)$  when  $k \in [-1, 1]$ ,  $\Delta s \in [-S_n^i, S_n^i]$ ,  $t \in [0, \tau_l]$ , (II) find the minimum of the function  $H(k, \Delta s, t)$  when  $k \in [-1, 1]$ ,  $\Delta s \in [-S_n^i, S_n^i]$ ,  $t \in [\tau_l, R_n^i]$ .

(I) Firstly, let us consider the function  $H(k, \Delta s, t)$  when  $k \in [-1, 1]$ ,  $\Delta s \in [-S_n^i, S_n^i]$ ,  $t \in [0, \bar{\tau}_l]$ ,  $0 < \bar{\tau}_l < \tau_l$ . From Proposition 2, we get

$$\begin{aligned} & \min_{k \in [-1, 1], \Delta s \in [-S_n^i, S_n^i], t \in [0, \bar{\tau}_l]} H(k, \Delta s, t) \\ &= \min \left\{ H(-1, -S_n^i, t_1), H(1, S_n^i, t_2), \right. \\ & \quad H(\max\{-1, \hat{k}_1\}, -S_n^i, \bar{\tau}_l), \\ & \quad \left. H(\max\{-1, \min\{\hat{k}_2, 1\}\}, S_n^i, \bar{\tau}_l), 0 \right\}, \end{aligned} \quad (\text{C.1})$$

where  $t_1, t_2, \hat{k}_1$  and  $\hat{k}_2$  are obtained in (22)-(25).

Since  $H(k, \Delta s, t) = \infty$  and  $H$  is continuous when  $(k, t) \neq (-1, \tau_l)$ , we have

$$\begin{aligned} & \min_{k \in [-1, 1], \Delta s \in [-S_n^i, S_n^i], t \in [0, \tau_l]} H(k, \Delta s, t) \\ &= \lim_{\tau_l^- \rightarrow (\tau_l)^-} \min_{k \in [-1, 1], \Delta s \in [-S_n^i, S_n^i], t \in [0, \bar{\tau}_l]} H(k, \Delta s, t). \end{aligned}$$

Moreover, denote

$$\begin{aligned} t_1^- &= \lim_{\bar{\tau}_l \rightarrow \tau_l^-} t_1, & t_2^- &= \lim_{\bar{\tau}_l \rightarrow \tau_l^-} t_2, \\ \hat{k}_1^- &= \lim_{\bar{\tau}_l \rightarrow \tau_l^-} \hat{k}_1, & \hat{k}_2^- &= \lim_{\bar{\tau}_l \rightarrow \tau_l^-} \hat{k}_2. \end{aligned}$$

It is easy to find that  $\hat{k}_1^- > -1$  and  $-1 < \hat{k}_2^- < 1$ . Thus, the minimum of  $H(k, \Delta s, t)$  for the case of (I) is

$$\begin{aligned} & \min_{k \in [-1, 1], \Delta s \in [-S_n^i, S_n^i], t \in [0, \tau_l]} H(k, \Delta s, t) \\ &= \min \left\{ H(-1, -S_n^i, t_1^-), H(1, S_n^i, t_2^-), \right. \\ & \quad \left. H(\hat{k}_1^-, -S_n^i, \tau_l), H(\hat{k}_2^-, S_n^i, \tau_l), 0 \right\}. \end{aligned} \quad (\text{C.2})$$

(II) Consider the function  $H(k, \Delta s, t)$  when  $k \in [-1, 1]$ ,  $\Delta s \in [-S_n^i, S_n^i]$ ,  $t \in [\tau^+, R]$ ,  $\tau^+ \in (\tau_l, R_n^i)$ . Since the function  $H(k, \Delta s, t)$  is a linear function

of  $\Delta s$ , the minimum is obtained at  $\Delta s = -S_n^i$  or  $\Delta s = S_n^i$ . Moreover, by Proposition 1, to obtain the minimum of the function  $H(k, \Delta s, t)$  on  $k$  and  $t$ , we only need to consider the two cases: (i)  $k \in [-1, 1]$ ,  $\Delta s = -S_n^i$ ,  $t \in [\tau^+, R_n^i]$ , (ii)  $k \in [-1, 1]$ ,  $\Delta s = S_n^i$ ,  $t \in [\tau^+, R_n^i]$ .

(i) Let  $\frac{\partial H(k, -S_n^i, t)}{\partial k} = 0$ , we get  $\hat{k}_1 \leq 0$  (see in (B.7)). Moreover,  $\hat{k}_1 \in [-1, 1]$  is equivalent to (B.9). Since  $t \geq \tau^+ > \tau$  and  $\left| \left(1 - \frac{S_n^i}{\hat{s}_n^i}\right)^{1/(\alpha+2)} - 1 \right| \leq 1$ , the inequality (B.9) holds. Thus, the minimum is obtained at  $k = \hat{k}_1$  and  $t = R_n^i$ .

(ii)  $H(k, S_n^i, t)$  is a convex function of  $k$ . Let  $\frac{\partial H(k, S_n^i, t)}{\partial k} = 0$ , we get  $\hat{k}_2$  (see (B.11)) and  $\hat{k}_2 \in [-1, 1]$  is equivalent to (B.14). From  $S_n^i \leq \hat{s}_n^i$  and  $\alpha > 0$ , we get  $0 \leq \left(1 + \frac{S_n^i}{\hat{s}_n^i}\right)^{1/(\alpha+2)} \leq 2$  which is equivalent to  $\left| \left(1 + \frac{S_n^i}{\hat{s}_n^i}\right)^{1/(\alpha+2)} - 1 \right| \leq 1$ . Since  $t \geq \tau^+ \geq \tau$ , the inequality (B.14) holds. Thus, the minimum is obtained at  $k = \hat{k}_2$  and  $t = R_n^i$ .

Thus, from (i) and (ii), we obtain

$$\begin{aligned} & \min_{k \in [-1, 1], \Delta s \in [-S_n^i, S_n^i], t \in [\tau^+, R_n^i]} H(k, \Delta s, t) \\ &= \min\{H(\hat{k}_1, -S_n^i, R_n^i), H(\hat{k}_2, S_n^i, R_n^i)\}. \end{aligned} \quad (\text{C.3})$$

Moreover, we have the following result:

$$\begin{aligned} & \min_{k \in [-1, 1], \Delta s \in [-S_n^i, S_n^i], t \in [\tau_l, R]} H(k, \Delta s, t) \\ &= \lim_{\bar{\tau}_l \rightarrow (\tau_l)^+} \min_{k \in [-1, 1], \Delta s \in [-S_n^i, S_n^i], t \in [\bar{\tau}_l, R]} H(k, \Delta s, t) \\ &= \lim_{\bar{\tau}_l \rightarrow (\tau_l)^+} \min\{H(\hat{k}_1, -S_n^i, R), H(\hat{k}_2, S_n^i, R)\}. \end{aligned} \quad (\text{C.4})$$

Denote

$$\begin{aligned} \hat{k}_1^+ &= \frac{\left( \left(1 - \frac{S_n^i}{\hat{s}_n^i}\right)^{1/(\alpha/2+1)} - 1 \right) \tau_l^2 - (R_n^i)^2}{2R_n^i \tau_l}, \\ \hat{k}_2^+ &= \frac{\left( \left(1 + \frac{S_n^i}{\hat{s}_n^i}\right)^{1/(\alpha/2+1)} - 1 \right) \tau_l^2 - (R_n^i)^2}{2R_n^i \tau_l}. \end{aligned}$$

Thus, the minimum of  $H(k, \Delta s, t)$  for the case of (II) is

$$\begin{aligned} & \min_{k \in [-1, 1], \Delta s \in [-S_n^i, S_n^i], t \in [\tau_l, R_n^i]} H(k, \Delta s, t) \\ &= \min\{H(\hat{k}_1^+, -S_n^i, R_n^i), H(\hat{k}_2^+, S_n^i, R_n^i)\} \\ &\leq \min\{H(\hat{k}_1^-, -S_n^i, \tau_l), H(\hat{k}_2^-, S_n^i, \tau_l)\}. \end{aligned} \quad (\text{C.5})$$

Therefore, from (C.2) and (C.5), we obtain

$$\begin{aligned} & \min_{k \in [-1, 1], \Delta s \in [-S_n^i, S_n^i], t \in [0, R_n^i]} H(k, \Delta s, t) \\ &= \min \left\{ H(-1, -S_n^i, t_1^-), H(1, S_n^i, t_2^-), \right. \\ & \quad \left. H(\hat{k}_1^+, -S_n^i, R_n^i), H(\hat{k}_2^+, S_n^i, R_n^i), 0 \right\}. \end{aligned} \quad (\text{C.6})$$

Base on Equations (B.1) and (C.6), we complete the proof.  $\square$

#### D Proof of Proposition 4

Note that the current remainder bound is  $\mathcal{B}_1^i \times \cdots \times \mathcal{B}_N^i$ . The remainder of  $f(\mathbf{x}) = \sum_{n=1}^N f_n(\mathbf{x}_n)$  (see (11)) is  $\Delta f = \sum_{n=1}^N \Delta f_n$  and  $\Delta f \in \mathcal{B}^i$  as shown in (8).

$\mathbf{x}_j \in \mathcal{E}_j^i$  is equivalent to  $\mathbf{x}_j = \hat{\mathbf{x}}_j^i + \hat{\mathbf{E}}_j^i \mathbf{u}_j$ ,  $\hat{\mathbf{x}}_j^i = [\hat{s}_j^i, (\hat{\rho}_j^i)^T]^T$ ,  $\hat{\mathbf{E}}_j^i = \begin{bmatrix} S_j^i & 0 \\ 0 & \mathbf{E}_j^i \end{bmatrix}$ ,  $\mathbf{E}_j^i$  is a Cholesky factorization of  $\mathbf{P}_j^i$ ,  $\mathbf{u}_j = [u_{1,j}, u_{2,j}]^T$ ,  $|u_{1,j}| \leq 1$ ,  $\|u_{2,j}\| \leq 1$ ,  $j = 1, \dots, N$ , then

$$s_n - \hat{s}_n^{i+1} = \hat{s}_n^i + S_n^i u_{1,j} - \hat{s}_n^{i+1}, \quad (\text{D.1})$$

$$\rho_n - \hat{\rho}_n^{i+1} = \hat{\rho}_n^i + \mathbf{E}_n^i u_{2,j} - \hat{\rho}_n^{i+1}. \quad (\text{D.2})$$

Denote  $\mathbf{y}^+$ ,  $f^+$  and  $\boldsymbol{\varepsilon}^+$  as shown in Proposition 4. We have

$$\begin{aligned} \mathbf{y}^+ &= f^+(\mathbf{x}) + \boldsymbol{\varepsilon}^+ \\ &= f^+(\hat{\mathbf{x}}^i) + \mathbf{J}^{+, (i+1)} \hat{\mathbf{E}}^i \mathbf{u} + \hat{\boldsymbol{\varepsilon}}^{+, i} + \mathbf{e}^{\boldsymbol{\varepsilon}, +} \\ & \quad + \text{diag}\left(\frac{\hat{\mathbf{b}}^{+, i} + \mathbf{b}^{\boldsymbol{\varepsilon}, +}}{2}\right) \Delta^+. \end{aligned} \quad (\text{D.3})$$

Moreover,

$$\begin{aligned} \mathbf{y}_l &= f_l(\mathbf{x}) + \boldsymbol{\varepsilon}_l \\ &= f_l(\hat{\mathbf{x}}^i) + \mathbf{J}^{l, (i+1)} \hat{\mathbf{E}}^i \mathbf{u} + \mathbf{e}_l^{\boldsymbol{\varepsilon}} \\ & \quad - \frac{b_l^{\boldsymbol{\varepsilon}}}{2} + D_l^{f, i} + \Delta_l, \end{aligned} \quad (\text{D.4})$$

where  $l \in \mathcal{L}^{-, i}$   $\mathbf{u} = [\mathbf{u}_1^T, \dots, \mathbf{u}_N^T]^T$ ,  $n = 1, \dots, N$ ,  $\Delta_{y_l} \geq 0$ .

If we denote  $\boldsymbol{\xi} = [1, \mathbf{u}^T, (\Delta^+)^T]^T$ , and  $\Phi_n^{s, (i+1)}$ ,  $\Phi_n^{\rho, (i+1)}$ ,  $\Psi^{+, (i+1)}$ ,  $\Psi_l^{-, (i+1)}$  are shown in (32)-(34), then (D.1),

(D.4) can be written as

$$s_n - \hat{s}_n^{i+1} = \Phi_n^{s, (i+1)} \boldsymbol{\xi}, \quad (\text{D.5})$$

$$\rho_n - \hat{\rho}_n^{i+1} = \Phi_n^{\rho, (i+1)} \boldsymbol{\xi}, \quad (\text{D.6})$$

$$0 = \Psi^{+, (i+1)} \boldsymbol{\xi}, \quad (\text{D.7})$$

$$\boldsymbol{\xi}^T \Psi_l^{-, (i+1)} \boldsymbol{\xi} \leq 0, l \in \mathcal{L}^{-, i}. \quad (\text{D.8})$$

Moreover, using (D.5)-(D.8) and  $\mathbf{x}_j = \hat{\mathbf{x}}_j^i + \hat{\mathbf{E}}_j^i \mathbf{u}_j$ ,  $\mathbf{u}_j = [u_{1,j}, u_{2,j}]^T$ ,  $|u_{1,j}| \leq 1$ ,  $\|u_{2,j}\| \leq 1$ ,  $j = 1, \dots, N$ , the conditions that  $\mathbf{x}_j \in \mathcal{E}_j^i$  and  $\Delta f_j(\mathbf{u}_j) \in \mathcal{B}_j^i$  are relaxed to

$$(\Phi_n^{s, (i+1)} \boldsymbol{\xi})^T (S_n^{i+1})^{-2} (\Phi_n^{s, (i+1)} \boldsymbol{\xi}) \leq 1, \quad (\text{D.9})$$

whenever

$$|\mathbf{u}_{1,j}| \leq 1, \quad (\text{D.10})$$

$$\|\mathbf{u}_{2,j}\| \leq 1, j = 1, \dots, N, \quad (\text{D.11})$$

$$|\Delta_l^+| \leq 1, l \in \mathcal{L}^{+, i}, \quad (\text{D.12})$$

$$\boldsymbol{\xi}^T ((\Psi^{+, (i+1)})^T \Psi^{+, (i+1)} \boldsymbol{\xi}) = 0, \quad (\text{D.13})$$

$$\boldsymbol{\xi}^T \Psi_l^{-, (i+1)} \boldsymbol{\xi} \leq 0, l \in \mathcal{L}^{-, i}, \quad (\text{D.14})$$

and

$$(\Phi_n^{\rho, (i+1)} \boldsymbol{\xi})^T (\mathbf{P}_n^{i+1})^{-1} (\Phi_n^{\rho, (i+1)} \boldsymbol{\xi}) \leq 1, \quad (\text{D.15})$$

whenever (D.10)-(D.14) are satisfied. The equations (D.10)-(D.14) are equivalent to

$$\boldsymbol{\xi}^T \text{diag}(-1, \text{diag}(\overbrace{0, \dots, \mathbf{I}_1, \dots, 0}^{\text{the } j\text{-th entry is } \mathbf{I}_1}), 0) \boldsymbol{\xi} \leq 0, \quad (\text{D.16})$$

$$\boldsymbol{\xi}^T \text{diag}(-1, \text{diag}(\overbrace{0, \dots, \mathbf{I}_2, \dots, 0}^{\text{the } j\text{-th entry is } \mathbf{I}_2}), 0) \boldsymbol{\xi} \leq 0, \quad (\text{D.17})$$

$$\boldsymbol{\xi}^T \text{diag}(-1, \text{diag}(\overbrace{0, \dots, 1, \dots, 0}^{\text{the } l\text{-th entry is } 1}), 0) \boldsymbol{\xi} \leq 0, \quad (\text{D.18})$$

$$\boldsymbol{\xi}^T ((\Psi^{+, (i+1)})^T \Psi^{+, (i+1)} \boldsymbol{\xi}) = 0, \quad (\text{D.19})$$

$$\boldsymbol{\xi}^T \Psi_l^{-, (i+1)} \boldsymbol{\xi} \leq 0, l \in \mathcal{L}^{-, i}. \quad (\text{D.20})$$

By S-procedure, a sufficient condition such that the inequalities (D.10)-(D.13) imply (D.9) to hold is that there exist scalars  $\tau^{y+}$  and nonnegative scalars  $\tau_j^1 \geq 0$ ,  $\tau_j^2 \geq 0$ ,  $j = 1, \dots, N$ ,  $\tau_l^+ \geq 0$ ,  $l \in \mathcal{L}^{+, i}$ ,  $\tau_l^- \geq 0$ ,  $l \in \mathcal{L}^{-, i}$ , such

that

$$\begin{aligned}
& (\Phi_n^{s,(i+1)})^T (S_n^{i+1})^{-2} (\Phi_n^{s,(i+1)}) - \text{diag}(1, 0, 0) \\
& - \sum_{j=1}^N \tau_j^1 \text{diag}(-1, \text{diag}(\overbrace{0, \dots, \mathbf{I}_1, \dots, 0}^{\text{the } j\text{-th entry is } \mathbf{I}_1}), 0) \\
& - \sum_{j=1}^N \tau_j^2 \text{diag}(-1, \text{diag}(\overbrace{0, \dots, \mathbf{I}_2, \dots, 0}^{\text{the } j\text{-th entry is } \mathbf{I}_2}), 0) \\
& - \sum_{l \in \mathcal{L}^{+,i}} \tau_l^+ \text{diag}(-1, \overbrace{0, \dots, 0, \dots, 0}^{\text{the } l\text{-th entry is } 1}) \\
& - \sum_{l \in \mathcal{L}^{-,i}} \tau_l^- \Psi_l^{-(i+1)} - \tau_{y^+} ((\Psi^{+,(i+1)})^T \Psi^{+,(i+1)}) \leq 0.
\end{aligned}$$

The following proof is similar to the proof of Theorem 3.1 in [34]. Thus, inequalities (D.9)-(D.14) are equivalent to (31).

In the same way, from (D.15) and (D.10)-(D.14), the problem (37)-(39) has been obtained. This completes the proof.  $\square$

## E Proof of Lemma 5

The problem of finding the lower bound  $\check{D}_{n,l}^i$  of the function  $f_{n,l}$  is equivalent to

$$\begin{aligned}
& \min \frac{s_n}{\|\rho_n - r_l\|^\alpha} \\
& \text{subject to } s_n \in \mathcal{E}_n^{s,i}, \rho_n \in \mathcal{E}_n^{\rho,i}, \alpha \in [\alpha_1, \alpha_2].
\end{aligned} \tag{E.1}$$

Since  $\frac{s_n}{\|\rho_n - r_l\|^\alpha}$  is a monotone function of  $s_n$  and  $\alpha$ , the problem (E.1) has the same optimal value with the following problem

$$\begin{aligned}
& \min \frac{\hat{s}_n^i - S_n^i}{\max\{\|\rho_n - r_l\|^{\alpha_1}, \|\rho_n - r_l\|^{\alpha_2}\}} \\
& \text{subject to } \rho_n \in \mathcal{E}_n^{\rho,i}.
\end{aligned} \tag{E.2}$$

In order to solve the problem (E.2), we only need to solve the following problem

$$\begin{aligned}
& \max \|\rho_n - r_l\| \\
& \text{subject to } \rho_n \in \mathcal{E}_n^{\rho,i}.
\end{aligned} \tag{E.3}$$

Similarly, we can obtain the upper bound  $\check{U}_{n,l}^i$  of the function  $f_{n,l}$ . This proves the lemma.  $\square$

## F Proof of Proposition 6

Since the function  $f_{l,n}(\mathbf{x}_n)$  is bounded by an interval  $[\check{D}_{l,n}, \check{U}_{l,n}]$ , for the  $n$ -th source, the measurement function is relaxed to

$$y_l = f_{l,n}(\mathbf{x}_n) + \hat{\varepsilon}_l, \quad l = 1, \dots, L, \tag{F.1}$$

where  $\hat{\varepsilon}_l \in [\hat{D}_{l,n}, \hat{U}_{l,n}]$ ,  $\hat{D}_{l,n} = \sum_{i \neq n} \check{D}_{l,i} + \mathbf{D}_\varepsilon(l)$ , and  $\hat{U}_{l,n} = \sum_{i \neq n} \check{U}_{l,i} + \mathbf{U}_\varepsilon(l)$ . Thus, for  $l = 1, \dots, L$ ,

$$\begin{aligned}
& \left( \max\left\{ \frac{y_l - \hat{U}_{l,n}^i}{g_l}, 0 \right\} \right)^{2/\alpha} \leq \frac{s_n^{2/\alpha}}{\|\rho_n - r_l\|^2} \\
& \leq \left( \frac{y_l - \hat{D}_{l,n}^i}{g_l} \right)^{2/\alpha}.
\end{aligned} \tag{F.2}$$

Since  $\alpha \in [\alpha_1, \alpha_2] \subset [2, 4]$  is unknown, (F.2) is relaxed to the following inequations, for  $l = 1, \dots, L$ ,

$$\check{D}_{n,l} \leq \frac{s_n^{2/\alpha}}{\|\rho_n - r_l\|^2} \leq \check{U}_{n,l}, \tag{F.3}$$

where  $\check{D}_{n,l}$  and  $\check{U}_{n,l}$  are defined in Proposition 6. For  $l = 1, \dots, L$ , we have

$$\|\rho_n - r_l\|^2 \geq \frac{s_n^{2/\alpha}}{\check{U}_{n,l}}. \tag{F.4}$$

For  $l \in \mathcal{L}^d$ , i.e.,  $\check{D}_{n,l} > 0$ , we get

$$\|\rho_n - r_l\|^2 \leq \frac{s_n^{2/\alpha}}{\check{D}_{n,l}}. \tag{F.5}$$

Denote  $\xi = [1, s_n^{2/\alpha}, \rho_n]^T$ . Thus, (F.4) is equivalent to

$$\xi^T \Phi_{n,l}^u \xi \leq 0, \tag{F.6}$$

and (F.5) is equivalent to

$$\xi^T \Phi_{n,l}^d \xi \leq 0, \tag{F.7}$$

where  $\Phi_{n,l}^u$  and  $\Phi_{n,l}^d$  are defined in (47) and (49).

For the  $n$ -th source,  $\mathbf{x}_n \in \mathcal{E}_n^i$ , and  $\alpha \in [\alpha_1, \alpha_2] \subset [2, 4]$ , we can check that

$$(\rho_n - \hat{\rho}_n^i)^T (\mathbf{P}_n^i)^{-1} (\rho_n - \hat{\rho}_n^i) \leq 1, \tag{F.8}$$

$$s_n^{2/\alpha} \in [D_n^s, U_n^s], \tag{F.9}$$

where  $D_n^s$  and  $U_n^s$  are defined in Proposition 6. The equations (F.8)-(F.9) are equivalent to

$$\xi^T \Phi_n^\rho \xi \leq 0, \quad \xi^T \Phi_n^s \xi \leq 0, \quad (\text{F.10})$$

where  $\Phi_n^\rho$  and  $\Phi_n^s$  are defined in (50) and (51).

The equations

$$|s_n^{2/\alpha} - \tilde{s}_n|^2 \leq \tilde{S}_n, \quad (\text{F.11})$$

$$(\rho_n - \hat{\rho}_n^{i+1})^T (\mathbf{P}_n^{i+1})^{-1} (\rho_n - \hat{\rho}_n^{i+1}) \leq 1, \quad (\text{F.12})$$

are equivalent to

$$\xi^T ((\Psi_n^s)^T \tilde{S}_n^{-1} \Psi_n^s - \text{diag}(1, 0, 0)) \xi \leq 0, \quad (\text{F.13})$$

$$\xi^T ((\Psi_n^\rho)^T (\mathbf{P}_n^{i+1})^{-1} \Psi_n^\rho - \text{diag}(1, 0, 0)) \xi \leq 0, \quad (\text{F.14})$$

where  $\Psi_n^s$  and  $\Psi_n^\rho$  are defined in Proposition 6.

By S-procedure, a sufficient condition such that the inequalities (F.4), (F.5) and (F.10) imply (F.13) to hold is that there exist nonnegative scalars  $\tau^1 \geq 0$ ,  $\tau^2 \geq 0$ ,  $\tau_l^3 \geq 0$ ,  $l = 1, \dots, L$ ,  $\tau_l^4 \geq 0$ ,  $l \in \mathcal{L}^d$ , such that

$$\begin{aligned} & (\Psi_n^s)^T s_{n,\alpha}^{-1} \Psi_n^s - \text{diag}(1, 0, 0) - \tau^2 \Phi_n^s \\ & - \tau^1 \Phi_n^\rho - \sum_{l=1}^L \tau_l^3 \Phi_{n,l}^u - \sum_{l \in \mathcal{L}^d} \tau_l^4 \Phi_{n,l}^d \preceq 0. \end{aligned} \quad (\text{F.15})$$

The following proof is similar to the proof of Theorem 3.1 in [34]. Thus, inequality (F.15) is equivalent to (54).

In the same way, a sufficient condition such that the inequalities (F.4), (F.5) and (F.10) imply (F.14) to hold is that the Equation (46) holds. This is the desired conclusion.  $\square$

## References

- [1] Y. Bar-Shalom. *Multitarget-multisensor tracking: advanced applications*. Norwood, MA, Artech House, 1990.
- [2] Y. Bar-Shalom, X. Li, and T. Kirubarajan. *Estimation with Applications to Tracking and Navigation*. New York: Wiley, 2001.
- [3] D. P. Bertsekas. *Nonlinear Programming*. Belmont: Athena scientific, second edition, 1999.
- [4] D. P. Bertsekas and I. B. Rhodes. Recursive state estimation for a setmembership description of uncertainty. *IEEE Transactions on Automatic Control*, 16:117–128, February 1971.
- [5] A. N. Bishop, B. Fidan, B. D.O. Anderson, K. Doğançay, and P. N. Pathirana. Optimality analysis of sensor-target localization geometries. *Automatica*, 46(3):479–492, 2010.
- [6] S. Boyd and L. Vandenberghe. *Convex Optimization*. Cambridge University Press, 2004.
- [7] A. Caiti, A. Garulli, F. Livide, and D. Prattichizzo. Localization of autonomous underwater vehicles by floating acoustic buoys: a set-membership approach. *IEEE Journal of Oceanic Engineering*, 30:140–152, 2005.
- [8] G. Calafiore. Reliable localization using set-valued nonlinear filters. *IEEE Transactions on Systems, Man, and Cybernetics-Part A: Systems and Humans*, 35(2):189–197, 2005.
- [9] G. Calafiore and L. El Ghaoui. Ellipsoidal bounds for uncertain linear equations and dynamical systems. *Automatica*, 40(5):773–787, 2004.
- [10] J. Chen, W. Dai, Y. Shen, V. K. N. Lau, and M. Z. Win. Power management for cooperative localization: A game theoretical approach. *IEEE Transactions on Signal Processing*, 64(24):6517–6532, 2016.
- [11] J. C. Chen, R. E. Hudson, and K. Yao. Maximum-likelihood source localization and unknown sensor location estimation for wideband signals in the near-field. *IEEE Transactions on Signal Processing*, 50(8):1843–1854, 2002.
- [12] Long Cheng, Chengdong Wu, Yunzhou Zhang, Hao Wu, Mengxin Li, , and Carsten Maple. A survey of localization in wireless sensor network. *International Journal of Distributed Sensor Networks*, 8(12):1–12, 2012.
- [13] C. Durieu, E. Walter, and B. T. Polyak. Multi-input multi-output ellipsoidal state bounding. *Journal of Optimization Theory and Applications*, 111(2):273–303, 2001.
- [14] M. L. Fowler and X. Hu. Signal models for TDOA/FDOA estimation. *IEEE Transactions on Aerospace and Electronic Systems*, 44(4):1543–1550, 2008.
- [15] A. Garulli and A. Vicino. Set membership localization of mobile robots via angle measurements. *IEEE Transactions on Robotics and Automation*, 17:450–463, 2001.
- [16] C.-Y. Han, M. Kieffer, and A. Lambert. Guaranteed confidence region characterization for source localization using RSS measurements. *Signal Processing*, 152:104–117, 2017.
- [17] L. Jaulin. A nonlinear set membership approach for the localization and map building of underwater robots. *IEEE Transactions on Robotics*, 25:88–98, 2009.
- [18] L. Jaulin, M. Kieffer, O. Didrit, and E. Walter. *Applied Interval Analysis: with examples in parameter and state estimation, robust control and robotics*. Springer Science & Business Media, 2001.
- [19] L. Jaulin, M. Kieffer, E. Walter, and D. Meizel. Guaranteed robust nonlinear estimation with application to robot localization. *IEEE Transactions on Systems, Man, and Cybernetics, Part C (Applications and Reviews)*, 32(4):374–381, 2002.
- [20] J. Löfberg. YALMIP: A toolbox for modeling and optimization in MATLAB. *Proceedings of the CACSD Conference*, 3:284–289, 2004.
- [21] M. Malanowski and K. Kulpa. Two methods for target localization in multistatic passive radar. *IEEE Transactions on Aerospace and Electronic Systems*, 48(1):572–580, 2012.
- [22] G. Mao and B. Fidan. *Localization Algorithms and Strategies for Wireless Sensor Networks*. IGI Global, 2009.
- [23] E. Masazade, R. Niu, P. K. Varshney, and M. Keskinöz. Energy aware iterative source localization for wireless sensor networks. *IEEE Transactions on Signal Processing*, 58(9):4824–4835, 2010.
- [24] G. Mellen, M. Pachter, and J. Raquet. Closed-form solution for determining emitter location using time difference of

- arrival measurements. *IEEE Transactions on Aerospace and Electronic Systems*, 39(3):1056–1058, 2003.
- [25] F. Meng, X. Shen, Z. Wang, and Y. Zhu. Set-membership multiple-source localization using acoustic energy measurements. In *20th IEEE International Conference on Information Fusion (Fusion)*, 2017.
- [26] W. Meng and W. Xiao. Energy-based acoustic source localization methods: a survey. *Sensors*, 17(2):376, 2017.
- [27] W. Meng, W. Xiao, and L. Xie. An efficient EM algorithm for energy-based multisource localization in wireless sensor networks. *IEEE Transactions on Instrumentation and Measurement*, 60(3):1017–1027, 2011.
- [28] R. Niu, R. S. Blum, P. K. Varshney, and A. L. Drozd. Target localization and tracking in noncoherent multiple-input multiple-output radar systems. *IEEE Transactions on Aerospace and Electronic Systems*, 48(2):1466–1489, 2012.
- [29] R. Niu, A. Vempaty, and P. K. Varshney. Received-Signal-Strength-Based localization in wireless sensor networks. *Proceedings of the IEEE*, 106(6):1166–1182, July 2018.
- [30] G. Piovana, I. Shames, B. Fidanc, F. Bulloa, and B. D. O. Anderson. On frame and orientation localization for relative sensing networks. *Automatica*, 49(1):206–213, 2013.
- [31] B. T. Polyak, S. A. Nazin, C. Durieu, and E. Walter. Ellipsoidal parameter or state estimation under model uncertainty. *Automatica*, 40(7):1171–1179, 2004.
- [32] F. C. Schweppe. Recursive state estimation: unknown but bounded errors and system inputs. *IEEE Transactions on Automatic Control*, 13(1):22–28, 1968.
- [33] I. Shames, B. Fidan, and B. D. O. Anderson. Minimization of the effect of noisy measurements on localization of multi-agent autonomous formations. *Automatica*, 45(4):1058–1065, 2009.
- [34] X. Shen, Y. Zhu, E. Song, and Y. Luo. Minimizing Euclidean state estimation error for linear uncertain dynamic systems based on multisensor and multi-algorithm fusion. *IEEE Transactions on Information Theory*, 57(10):7131–7146, 2011.
- [35] X. Sheng and Y.H. Hu. Maximum likelihood multiple-source localization using acoustic energy measurements with wireless sensor networks. *IEEE Transactions on Signal Processing*, 53(1):44–53, 2005.
- [36] P. Strumillo. *Advances in Sound Localization*. InTech, 2011.
- [37] Y. Theodor, U. Shaked, and C. E. de Souza. A game theory approach to robust discrete-time  $h_\infty$  estimation. *IEEE Transactions on Signal Processing*, 42:1486–1495, 1994.
- [38] A. Vempaty, Y. S. Han, and P. K. Varshney. Target localization in wireless sensor networks using error correcting codes. *IEEE Transactions on Information Theory*, 60(1):697–712, 2014.
- [39] A. Vempaty, O. Ozdemir, K. Agrawal, H. Chen, and P. K. Varshney. Localization in wireless sensor networks: Byzantines and mitigation techniques. *IEEE Transactions on Signal Processing*, 61(6):1495–1508, 2013.
- [40] X. Wang, B. Quost, J.-D. Chazot, and J. Antoni. Estimation of multiple sound sources with data and model uncertainties using the EM and evidential EM algorithms. *Mechanical Systems and Signal Processing*, 66–67:159–177, 2016.
- [41] M. Z. Win, W. Dai, Y. Shen, G. Chrisikos, and H. Vincent Poor. Network operation strategies for efficient localization and navigation. *Proceedings of the IEEE*, 106(7):1224–1254, 2018.
- [42] H. S. Witsenhausen. Sets of possible states of linear systems given perturbed observations. *IEEE Transactions on Automatic Control*, 13(5):556–558, 1968.
- [43] Y. I. Wu and K. T. Wong. Acoustic near-field source-localization by two passive anchor-nodes. *IEEE Transactions on Aerospace and Electronic Systems*, 48(1):159–169, 2012.
- [44] H. Wymeersch, J. Lien, and M. Z. Win. Cooperative localization in wireless networks. *Proceedings of the IEEE*, 92(2):427–450, 2009.
- [45] W. Yu, E. Zamora, and A. Soria. Ellipsoid slam: a novel set membership method for simultaneous localization and mapping. *Autonomous Robots*, 40:125–137, 2016.
- [46] S. A. Zekavat and R. M. Buehrer. *Handbook of Position Location: Theory, Practice and Advances*. John Wiley & Sons, 2011.
- [47] X. Zhang, L. Xu, and L. Xu. Direction of departure (DOD) and direction of arrival (DOA) estimation in MIMO radar with reduced-dimension MUSIC. *IEEE Communications Letters*, 14(12):1161–1163, 2010.
- [48] Y. Zhu. *Multisensor Decision and Estimation Fusion*. Kluwer Academic Publishers, Boston, 2003.